3-16-2016

Analysis and Processing of Human Electroretinogram

Abdulrahman Mohammad Alaql

Analysis and Processing of Human Electroretinogram

by

Abdulrahman Alaql

A thesis submitted in partial fulfillment
of the requirements for the degree of
Master of Science in Electrical Engineering
Department of Electrical Engineering
College of Engineering
University of South Florida

Major Professor: Wilfrido Moreno, Ph.D.
Alexandro Castellanos, Ph.D.
Ismail Uysal, Ph.D.

Date of Approval:
March 11, 2016

Keywords: Wavelet, Glaucoma, Photopic, ERG, Retina, i-wave, PhNR

DEDICATION

I dedicate my thesis work to my loving family and friends. A special feeling of gratitude to my amazing parents, Mohammad and Abeer, whose words of encouragement and push for tenacity ring in my ears. My brothers and sisters are also to thank due to their love and support. I also dedicate this thesis to my friends who have supported me throughout the process which made it easier for me to achieve my goals. I will always appreciate all they have done, especially Ammar and Abdullah who were always cheerful and positive towards every decision I made regarding this study. I finally dedicate this work and give special thanks to my wife and best friend Asmaa, for being there for me throughout the entire master program, who helped me become more confident and optimistic, and who made it easier for me to do this thesis through her love and support. You really are wonderful.

ACKNOWLEDGEMENTS

I would like to thank my committee members who were very helpful and supportive with their expertise, inputs and time. A special thanks to Dr. Wilfrido Moreno, my committee chairman for his hours of reading, encouraging, and most of all patience throughout the entire process. I would also like to acknowledge and thank the electrical engineering department for allowing me to conduct my research and providing any assistance requested. Special thanks goes to Dr. Radouil Tzekov and Mr. Prashanth Chetlur Adithya, their excitement and willingness to provide feedback made the completion of my thesis both an enjoyable and beneficial experience.

TABLE OF CONTENTS

LIST OF TABLES

LIST OF FIGURES

ABSTRACT

Electroretinagram (ERG) is the recording of electrical activity of retinal cells elicited by light stimulation, which has been widely used to help diagnose different types of retinal dysfunctions. The ERG response signal is a short non-stationary signal that contains overlapping components. Different Digital Signal Processing (DSP) techniques are investigated using MATLAB to study the time-frequency responses of the ERG signal such as Short Time Fourier Transform (STFT), Continuous Wavelet Transform (CWT) and Discrete Wavelet Transform (DWT). The Photopic ERG signal was processed and analyzed in this thesis and the results of each technique have been investigated in detail. The Photopic ERG components have been extracted using DWT and ERG Models.

CHAPTER 1: INTRODUCTION

1.1 Problem Statement

This thesis will cover the area of digital signal processing analysis of the Electroretinogram (ERG) response of the human eye, focusing on the methods that can be used to extract useful analytical information. These information help identify abnormal behaviors in the patient eyes which can lead to an improved diagnosing process. These performed tests if analyzed properly could also have the potential to predict future problems relating to retinal disorders [1].

Early detection of retinal disorder by ERG analysis has been an area of study since 1965 [2]. The diagnostic procedures and methods which have been used in the field still have large room for improvement. The test speed and number of samples taken are significant, also the processing time and efficiency are a factor that will largely affect the performance of the diagnostic system and ease the process for testing subjects and patients [3].

The ERG is considered as a mass recording of various responses of different cells in the retina, these responses are basically formed by stimulating the retinal cells [3]. The ERG signal contains different components that are driven by different sources in the retinal structure. Some of these components are present in most ERG signals such as a-wave and b-wave, other components such as i-wave and Photopic Negative Response (PhNR) are only present in specific conditions regarding the data collection method [4]. Most of ERG components have not been standardized since they are still challenged in regard of their origins in medical trials [5]. Hence,

ERG components are not completely explored and the physiological interpretations for these components are also to be standardized.

Recent research focuses on the time domain analysis of the ERG signal and more specifically on the early response which consist of a-wave and b-wave. The need of applying different methods and techniques of signal processing which can offer additional details of the ERG that can help to study the different ERG signal components has been identified. Hence, this thesis presents the study, the comparison and the analysis of using different techniques of signal processing in ERG signals. The extracted ERG information will help expand the knowledge of ERG components as well as the assessment of eye status and retinal condition.

1.2 Thesis Objective

The goal of this thesis is to understand the significance of ERG response and its characteristics as well as to introduce signal processing approaches to extract essential information from the ERG signal. Different signal processing methods are carefully applied using processing tools such as Short Time Fourier transform (STFT), Continuous Wavelet Transform (CWT) and Discrete Wavelet Transform (DWT). The output of these transforms have been analyzed and compared in order to choose the most efficient approach with best realistic measurements and acceptable resolution. Additionally, a signal decomposition approach using DWT has been developed to isolate different components in ERG, and the detailed analysis of the decomposed signals is provided.

1.3 Thesis Outline

This thesis is organized as follows. In Chapter 2, the ERG fundamentals are discussed. In Chapter 3, the DSP methods used in this thesis are introduced with the state of the art of each

approach. Chapter 4 shows the results of the introduced DSP. In Chapter 5, the overall results are discussed in detail. In Chapter 6, contributions are summarized and an outline for open issues and future work is presented.

CHAPTER 2: BACKGROUND

Electroretinagram testing has been used in humans and laboratory animals since the late nineteen forties under the influence of Swedish pioneers Holmgren and Granit [1]. Typically, the test determines the retinal status and acts as a check for retinal diseases and dysfunctions. The ERG is basically a mass response of the eye's retina after the simulation of a bright light. The applied light causes the retina to produce a response measured in voltage, which is addressed as ERG [1].

The method of recording the eye response is by stimulating the eye with a flash or a bright light and record the response using a recording electrode attached to the patient's eye. The test is usually repeated multiple times and the response is averaged in order to obtain an accurate and clutter free signal [2]. Various retinal cells and tissues respond to the stimulation and is recorded in the ERG test. These cells and tissues react differently and produce unique selective responses. Hence, ERG signal has a highly diagnostic potential [8]. The length of ERG signal is typically 200 milliseconds, being the first 80 milliseconds the most essential time segment as it contains most of the ERG components. This suggests that the ERG signal is relatively a short signal, and provides a significant challenge to the analysis of the signal. Figure 1 shows an ERG response signal. The retina typically has about 120 million rods and about 6 million cones which suggests that the response of the ERG will be dominated by rods. The rods and cones responses can be isolated using different test settings such as manipulating colors, amplitudes and intensity of the light simulator in the testing condition.

The reason for obtaining isolated responses is because each response can give more accurate measurements of a-wave and b-wave amplitudes and respective peak times while these measurements can only be obtained by isolating the response from cones and rods [9]. One method of isolating rods and cones is by controlling the wavelength (color) of simulated light. The peak wavelength sensitivity for rods is around 510 nm, also known as Scotopic Response, while the peak wavelength sensitivity for cones is 560 nm, defined as the Photopic Response [10].

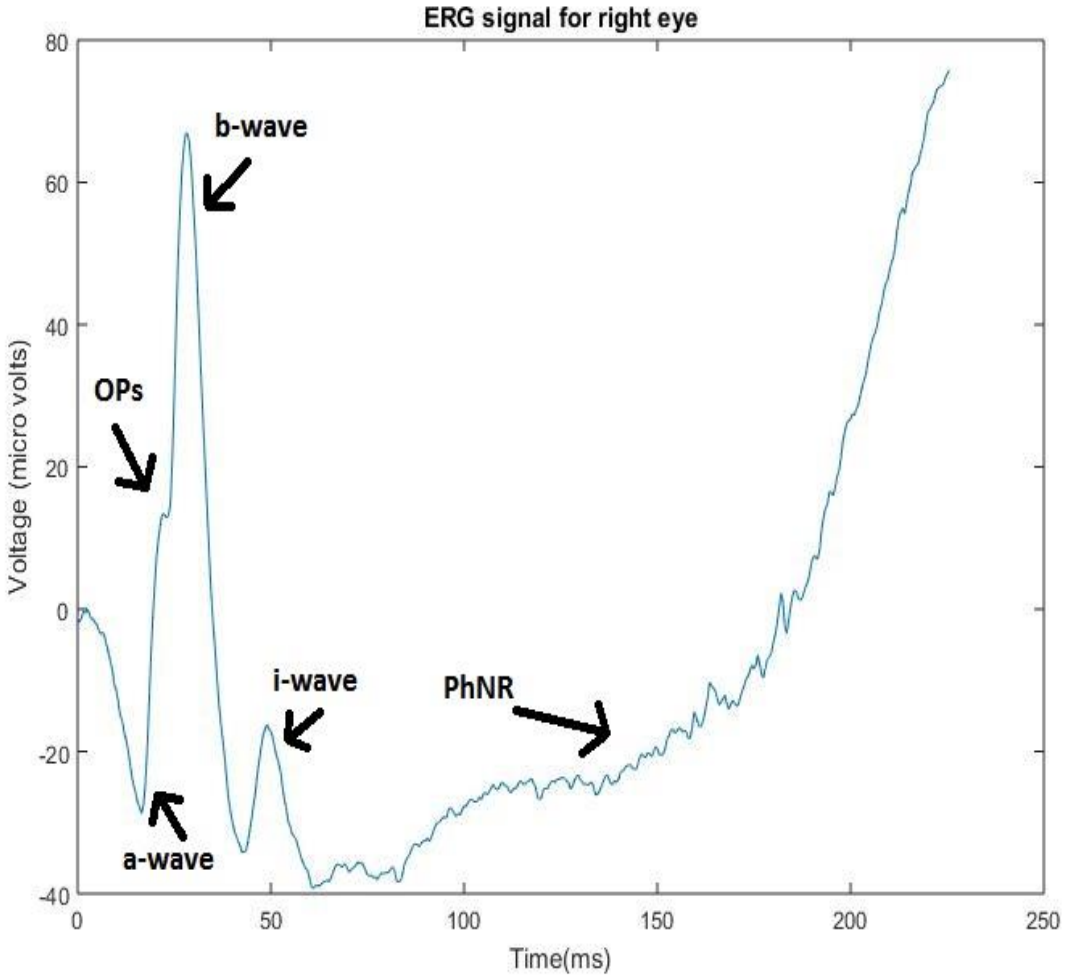

Figure 1: ERG Photopic Response

As shown in Figure 1, the two main components in ERG responses are the a-wave and b-wave. The a-wave is the first negative wave and the b-wave is the positive wave which directly follows the a-wave and usually has a high positive amplitude. Both components are essential in ERG testing as they are usually measured in amplitude and time to determine retinal status [6]. Following these two components, i-wave and photopic negative response are also shown in figure 1, however these two components are not always present. The following sections provide more details regarding each ERG component.

2.1 ERG Component: the a-wave

The a-wave originates from the cones and the rods of the retina and is the first visual response of the ERG signal [9]. The a-wave usually determines the physiological health of the retina photoreceptors [9].The standard features of a-wave are the negative trough, the amplitude from the baseline to the a-wave trough and the time from the light onset to the trough of a-wave. Characteristics of a-wave highly depend on the type of the ERG response, a-wave can have different features if the applied ERG test is configured to attract either cones or rods [10]. In the photopic ERG response, a-wave is a measure of the outermost retinal layer [10].

2.2 ERG Component: the b-wave

The b-wave is formed by the ON bipolar cells of the retina [9], but other studies suggest that there is a contribution to the response from the Muller cells [11]. The features of b-wave mainly focuses on the peak-to-peak amplitude from the peak of the b-wave to the trough of the a-wave and on the time measured from the light onset to the time when the b-wave peaks. The b-wave determine the health of the inner layers of the retina [7]. Unlike a-wave, b-wave does not significantly change in shape in regard to cone or rod dominant ERG signals [10].

2.3 ERG Component: the i-wave

As shown in figure 1, the i-wave is an ERG component that is present as the positive increase after the b-wave, it appears in the photopic ERG response. The i-wave does not appear in all ERG test settings, which suggests that it could only be a cone related response. The i-wave is initiated if the ERG photopic response when a light intensity setting is optimized to attract cones. This component appears as a small positive hill stationed around 50 ms which will start descending afterwards as the PhNR starts to appear [11]. The i-wave is believed to be originated in the inner retina and specifically in the RGCs. There have not been many studies regarding the i-wave and its significance nor extracting of i-wave and PhNR signals using time and frequency analysis [5].

The i-wave is believed to originate from the inner part of the retina. However, this observation has been challenged [11] and there is no research evidence regarding the physiological significance of the i-wave and its direct association to retinal disorders. I-wave features include the implicit time at which the i-wave peaks and its respective peak amplitude from the ERG baseline [13].

2.4 Photopic Negative Response

The photopic negative response (PhNR) in an ERG is the negative wave following the b-wave. The PhNR is driven by the retinal ganglion cells (RGCs). The analysis of this negative response determines diseases in the retina caused in RGCs, also it can be a functional test for the optical nerve in the retina [10]. There are few studies in the literature regarding exploring the PhNR and i-wave features, the explored analysis of these components were only focused on the signal in time domain. The PhNR features include the difference between the most negative

voltage after the tail of the i-wave and the baseline (zero volt), there are other applied approaches which are less affected by noise such as determining the lowest negative voltage level of the PhNR and the time where the ERG component is initiated [13]. The ERG response in glaucoma patients shows a reduction in the PhNR amplitude which elevates the i-wave and makes it more detectable [12]. This observation shows the importance of analyzing this response and use it to improve glaucoma diagnostic procedures.

2.5 Oscillatory Potentials

The Oscillatory Potentials (OPs) are formed by the Amacrine cells in the inner retina. They are the potentials following the b-wave, usually they are at a higher frequency than all other ERG components and less in amplitude. The OPs are attenuated in many retinal diseases such as Retinitis Pigmentosa, diabetic retinopathy and several other conditions [9].

Table 1: Summary of Photopic ERG Components

ERG Components	Origin	Component Features	Existence Time	Existence Frequency Band
a-wave	Cones and Rods	Negative First Trough	Transient (Early Response)	Wide Band
b-wave	ON Bipolar Cells and Muller Cells	Positive Highest Peak	Transient (Early Response)	Wide Band
i-wave	RGC	Negative peak between b-wave and PhNR	Exists Across Entire ERG	Wide Band
PhNR	RGC	Ascending from lowest amplitude after i-wave	Exists Across Entire ERG	Narrow Band
OPs	Amacrine Cells	Low amplitude Oscillations Across the ERG	Exists Across Entire ERG	Narrow Band

In conclusion, a-wave and b-wave have only been explored in time domain and their features are defined in terms of amplitudes and implicit times. OPs are explored in the literature and are extracted by filtering the ERG response. The exact definition of i-wave and PhNR noticeably varies in the literature, which makes the related research to i-wave and PhNR very limited and this thesis will apply different processing methods that can help make a contribution in the regard of PhNR and i-wave components [16]. Frequency domain characteristics of ERG components have not been explored in details. In Table 1, a summary of photopic ERG components is presented.

CHAPTER 3: STATE OF THE ART

This chapter will elaborate on the methodologies used to obtain and analyze the ERG signal. It begins with the process of data collection and how it affects the obtained signal, and presents the types of ERG responses based on various configurations applied to the testing process. This chapter will then identify each signal processing technique used in this thesis, with the application of each technique being focused on ERG signals. Finally, ERG mathematical models that have been developed to represent an ERG response with different configurable parameters.

3.1 ERG Data Collection Process

The standard method used for ERG data collection is through applying a flash pulse directed to the subject's eye, and recording the captured response. A staged process is performed in order to obtain the optimum response, each stage will be discussed in this section. Figure 2 is the representation of the staged process for the ERG data collection.

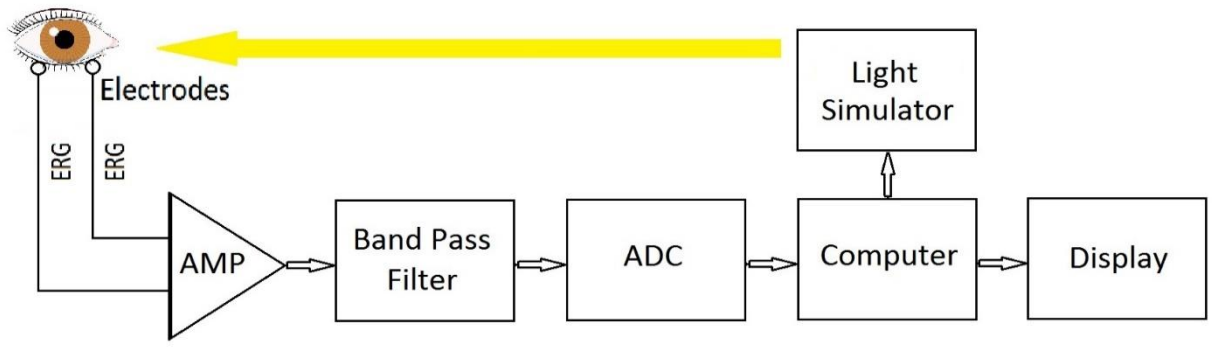

Figure 2: ERG Data Collection Block Diagram

The ERG data collection process uses a digitally controlled device that can be attached to the subject's eye through a number of electrodes [8]. There are different methods to record the ERG response, the most popular is by using a ring wire attached to a contact lens and placed on the pupil. Usually the eye will be held open using speculum structures to avoid eye movements and blinking during the test. Another type of electrode used can be made with a cotton wick. The controlling unit of the device is a computer, this computer is responsible for initiating the test by triggering a timed pulse of light through a strobe light source. The light source is directed to the subject's eye and the electrodes are connected to the subject's pupil where the retina is connected, which is light sensitive and located in the back tissue of the eye. After the light rays passes the cornea, pupil and lens, they are focused onto the retina. The retina receives these rays and converts them to electrical signals that are passed to the brain through optic nerves [5]. An ERG response is generated and captured by the electrodes, and the electrodes are connected to an amplifier which can scale the response to a readable level. A band pass filter is used to remove undesired frequencies, the filter's bandwidth used in this application is typically 0.3 Hz-500 Hz [18]. An analog to digital converter captures the filtered signal in order to send it to the processing unit. The computer is then used for displaying the ERG response in time domain using a display unit. It can also store data for further analyis, capture multiple ERG signals and average them in order to remove noise [18]. Depending on the setting of the light color and intensity and the onset period, a response can either be a Scotopic or a Photopic ERG signal.

In each case, some ERG components can be shaped differently, other components may not be present, such as i-wave and PhNR which can only be present in the Photopic ERG response. Photopic ERG can be achieved by a bright high intensity flash stimulation for a short

period of time. Databases of ERG signals can be a useful source of data of different ERG types and different subjects. However, there are no publicly available databases for ERG signals.

3.2 ERG Signal Processing

The approach of exposing the ERG signal to different signal processing techniques can start with basic steps such as time domain analysis as well as frequency domain analysis. More complex techniques will be then used in this study to extract additional information from the signal in order to obtain better accuracy. The Short Time Fourier Transform (STFT) will be performed as well as the Continuous Wavelet Transform (CWT) and the Discrete Wavelet Transform (DWT). The STFT and CWT techniques will have some similarities in the output, however expected differences are found with respect to accuracy and resolution. The output of these two methods will be compared and analyzed.

3.2.1 Short Time Fourier Transform

The standard Fourier transform will show the frequency spectrum of the entire signal. The limitation of this approach is that the frequency parameters of the signal in a specific time cannot be determined. Hence, the short time Fourier transform is a suggested approach to analyze the ERG signal in a time-frequency domain.

Short time Fourier transform, or also known as windowed Fourier transform, is the approach of dividing the signal into short segments of equal length of time. Each segment of time shall be evaluated individually and the resulting frequency content of each segment can be displayed under that period. As shown in Figure 3, the resolution of the short time Fourier transform depends mainly on the length of the segment, i.e. a shorter segment in time will result

in a lower frequency resolution which reflects as a wider segment in the frequency domain. Figure 3 shows two different types of STFT.

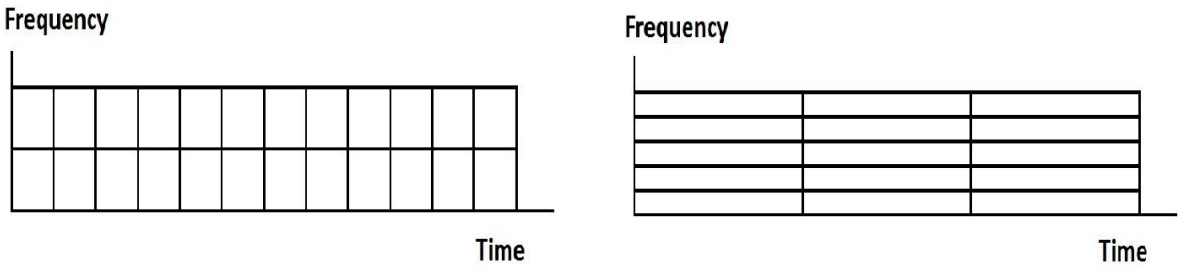

Figure 3: Time and Frequency Resolution of Short Time Fourier Transform

As shown in Figure 3, the segments chosen for a particular time resolution (left) has a poor frequency resolution, while obtaining a better frequency resolution (right) will result in lower resolution in time. This approach of analyzing the ERG signal using the short time Fourier Transform has not been used to analyze ERG responses [16]. The outcome of the Short Time Fourier Transform will usually be displayed in a two dimensional plot with time in the x-axis and frequency in the y-axis. The amplitude of the transformed signal will be represented as the color of the signal with a color index that shows the difference between high and low amplitude values. The STFT major disadvantage is that it mainly depend on the signal's resolution and sampling frequency.

3.2.2 Wavelet Transform

The wavelet transform is another type of time-frequency representation of a signal. There are two types of wavelet transforms, a continuous wavelet transform and a discrete one. The wavelet transform is usually performed in both forms to obtain more information and better result. Continuous Wavelet Transform and Discrete Wavelet Transform are used to analyze and

display the time-scale plot of a signal. Additionally, they are used to decompose the signal into its original components. The following sections will briefly explain the concept of the wavelet transform and what has been described in the literature to analyze the ERG signal.

3.2.2.1 Continuous Wavelet Transform

The continuous wavelet transform is achieved by the convolution of the given signal with a series wavelets. Those wavelets are shifted and stretched in time domain. The wavelet function used to generate the series is called the mother wavelet, and the generated series of wavelets are called the daughter wavelets. The process of shifting the series of wavelets with the original signal is called translation, and the process of scaling the wavelet is called dilation. The result of the translation and dilation is a series of coefficients that are acting as a quantitative representation of the similarity relation between the signal and the series of translated and dilated wavelets [18].

The coefficients of the continuous wavelet transform are plotted against the scales of the transform. Those scales are translated into pseudo approximated frequency values which will be used to generate a time versus frequency plot [19].

Mathematically, the wavelet coefficient equation is given by the following:

$$Coefficient\ \ C(a,b) = \int_{-\infty}^{+\infty} x(t)\psi_{a,b}(t)dt \qquad (1)$$

The coefficient C in equation 1 is the similarity value, which means the higher the value, the more similar the wavelet to the original signal, and the lesser the value means the wavelet is not similar [19].

In equation 1, the function $\psi_{a,b}(t)$ is the mother wavelet which is represented as:

$$\psi_{a,b}(t) = a^{-\frac{1}{2}}\psi\left(\frac{t-b}{a}\right) \qquad (2)$$

The wavelet $\psi(t)$ in equation 2 is being parameterized by a and b, where a is the scale of the wavelet and b is the translation parameter or the shift value of the wavelet. Each coefficient is convolving the original signal with the mother wavelet which is treated with the scale and the translation parameters [20].

Various wavelets can be used for performing the transform for ERG signals. The first suggested wavelet is the Haar wavelet which is the most basic since it consists of a positive pulse followed by a negative pulse of the same amplitude and period. Haar wavelet is mostly suited for digitally acquired signals since it is one of the few wavelets with sharp edges that can detect discontinuity. Other wavelets that can be used in this application are Daubechies, Mexican Hat, and Morlet [19] [21] [22]. Those wavelets have been used for ERG signal analysis.

The use of continuous wavelet transform in ERG signals is essential since the ERG signal is the superposition of different components [9] (based on Granit's model) with different frequencies and amplitudes, initiated in different times and delays. The continuous wavelet transform can help clarify the frequency band of each component.

Choosing a suitable wavelet and scales values are key to obtaining a more accurate result. A comparison of the continuous wavelet transform and the short time Fourier transform can work as a verification of wavelet transforms being performed accurately, which will result in more confident findings regarding the ERG signal analysis.

The Continuous Wavelet Transform (CWT) has some limitations and constraints which makes it difficult to analyze the signal using this approach. Mainly, this happens because of the wavelet coefficients are affected by the choice of the wavelets and the values of scales [15]. Also the repetitive process and redundant outcomes are considered as a downside, which makes the transform require a great amount of computation power and time. Therefore, the discrete wavelet transform is developed [35]. The reconstruction process of CWT is limited to linearly scaled coefficients, and the accuracy of the reconstructed signal is not always acceptable. Cone of influence is also a factor that can affect the result of the transform, this occurs when a signal has a high impulse and the transform considers that impulse as a high frequency value. Hence, the signal is affected by the cone of influence if the signal is transformed using the convolution based CWT.

3.2.2.2 Discrete Wavelet Transform

The Discrete Wavelet Transform (DWT) is the process of digitally decomposing an input signal, the transform was developed by Mallat in 1989 [35]. The discrete wavelet transform is achieved by performing a signal decomposition algorithm using high pass filters and low pass filters, and followed by a down sampling stage after each filtering step. The transform aims to decompose the signal by performing a frequency banding process which isolate the content of the signal in each specific frequency band based on the wavelet chosen and the level of decomposition. A bank of filters is used to achieve the transform. The output of each high pass filter is called an approximation signal, and the output of each low pass filter is called a detail signal [35].

The input signal is run through two different filters, a low pass filter and a high pass filter. Both filters have the same cutoff frequencies and the original signal is split in half in

terms of frequency band. Both outputs from the filters are run through a down sampling stage. The resulting two signals are the output of the first stage of decomposition. This process is repeated for each down sampled output and the number of stages determines the wavelet transform frequency resolution. The frequency is also divided in each stage since the filtering limits the bands. The reason of applying the filters is to reduce the frequency bandwidth in order to achieve coefficients with better frequency resolution. Mathematically, the coefficient equation for the discrete wavelet transform is given by equation 3:

$$C(a,b) = C(j,k) = \sum_{n} x(n)\psi_{j,k}(n) \qquad (3)$$

C in equation 3 is the coefficient function which is representing the discrete method of computing the similarity between two functions. The parameters j and k are the power values of the base 2 in a and b respectively [35].

$$\psi_{j,k}(n) = 2^{-\frac{j}{2}}\psi(2^{-j}n - k) \qquad (4)$$

The wavelet function in equation 4 is represented as the original function parameterized to change in scale by the parameter j and shifted by the parameter k.

The values of shifted wavelets have to be integers since the function is discrete, therefore the more samples in the original signal would cause the coefficients to be in better resolution.

Different wavelets can be very useful to treat the ERG signal. Although, the factor of choosing a suitable wavelet can affect the outcome, there are many wavelets that can be applied to give a good resolution and a realistic measurement.

One of the most important wavelets used in discrete wavelets transform is the Daubechies wavelet. This wavelet has many members that can give different response in the transform. The higher the member value, the smoother the signal is. The Daubechies wavelet is commonly used in the discrete wavelet transform because of its balanced number of vanishing moments. Another good reason for using this wavelet in this research is that the Daubechies wavelet is very similar to the ERG signal, this means that the coefficients of the transform will show better (higher) values in the large scales (low frequencies) which result in more accurate transform and decomposition process [16]. Other wavelets have been used for ERG signal analysis in DWT are Symlets [17].

The fact that discrete wavelet transform is a practical approach, it is because it can be easily applied to most types of signals, it also has a very efficient performance with lower computation power and time. And more importantly, it is easily reconfigurable and adjustable for this type of study [32].

DWT approximation and detail signals can be reconstructed to reform the original signal. The reconstruction process is performed by simply adding all the decomposed signals resulted from the wavelet transform and comparing it with the original ERG signal. The difference between reconstructed and original signals occurs due to the performance of digital filters used by the transforming tool [31]. The reconstructed signal is useful for comparing the original signal with the decomposed components of the transform. The analysis of the wavelet transform will briefly touch the subject of comparing the original signal with the reconstructed one.

3.3 ERG Models

The model used in this study for ERG signal analysis has been developed by J.Castro [43]. This model has been obtained to represent the ERG response mathematically and graphically based on different factors such as light latency and intensity. Castro's model is used in this research to generate an ERG signal consisting of a-wave and b-wave in order to decompose the signal by removing the modeled waves from the original response. The following mathematical equation represents Castor's ERG model of a-wave and b-wave.

$$ERG(t) = A(t) + B(t) \tag{5}$$

Equation (5) shows that the ERG model consists of the superimposition of $A(t)$ and $B(t)$ models in time domain, where all parameters are a function of time.

$$A(t) = K_1 . \left[1 - e^{-\alpha_1 . \left[\left(t / t_P \right) . e^{\left[1 - \left(t / t_P \right) \right]} \right]} \right] \tag{6}$$

Equation (6) represents the model of a-wave, where K_1 is a-wave amplitude, α_1 is the light intensity factor, t_P is the peak time of a-wave.

$$B(t) = K_2 \, . \, t^3 \, . \, e^{-\alpha_2 . t} \, . \, \sin (\omega . t) \tag{7}$$

Equation (7) shows the b-wave model. Where K_2 is the peak amplitude, α_2 is the light intensity factor and ω is the peak location which is represented as the shift of the sinusoid's peak.

In conclusion, this chapter discussed the methods of collecting ERG data, signal processing techniques to analyze the data, and models used for analyzing ERG signals. Each technique has been explored and linked to ERG signal analysis, challenges and limitations of each technique has also been discussed.

CHAPTER 4: RESULTS

This chapter will elaborate on the results of the discussed ERG signal analysis methodologies in this thesis. The main software tool being used for this chapter is MATLAB and a step by step process has been performed to produce more comprehensive measurements. Time domain analysis of the signal is the basic first step in observing ERG data. Although the time domain analysis has always been the standard ERG evaluation method [27], it can be a useful step to perceive different characteristics of the response.

Following the time domain analysis, frequency domain analysis is to be presented using Fourier transform. The frequency spectrum of the ERG signal can give a clear insight on the centered frequency and the power of the signal in different frequency bands.

The short time Fourier transform is also to be implemented and analyzed in this chapter, as well as the continuous wavelet transform. A brief comparison between short time Fourier transform and continuous wavelet transform will be described. Finally, the most essential stage of this study is applying the discrete wavelet transform, which can offer much more details and the ability to decompose the ERG signal into its frequency components.

4.1 Obtained ERG Signal

The presented ERG signal used in this thesis is obtained from a healthy male subject in his mid-forties. The ERG is a cone-driven response which is specified as the ERG photopic response. The receiving electrodes have been attached to the eye pupils and a sudden short

bright flash is stimulated in order to obtain the photopic ERG. The background of the test area is of white color and the only light source in the testing period was the flash. The test has been repeated for both eyes, each eye has been tested ten times. Those ten signals have been averaged to remove noise and unwanted spikes. The resulting averaged signal has been sampled by a 2000 Hz sampling frequency. The resolution of the ERG signal is 16 bit and the baseline is 0v.

4.2 ERG in Time and Frequency Domain

The ERG response is a 16-bit-resolution signal with a 2000 Hz sampling frequency; the signal has been averaged from 10 raw captured responses in order to reduce noise. As shown in figure 4, the first negative peak and the following positive peak (a-wave and b-wave) are measured from the base line and the implicit time from t=0 ms.

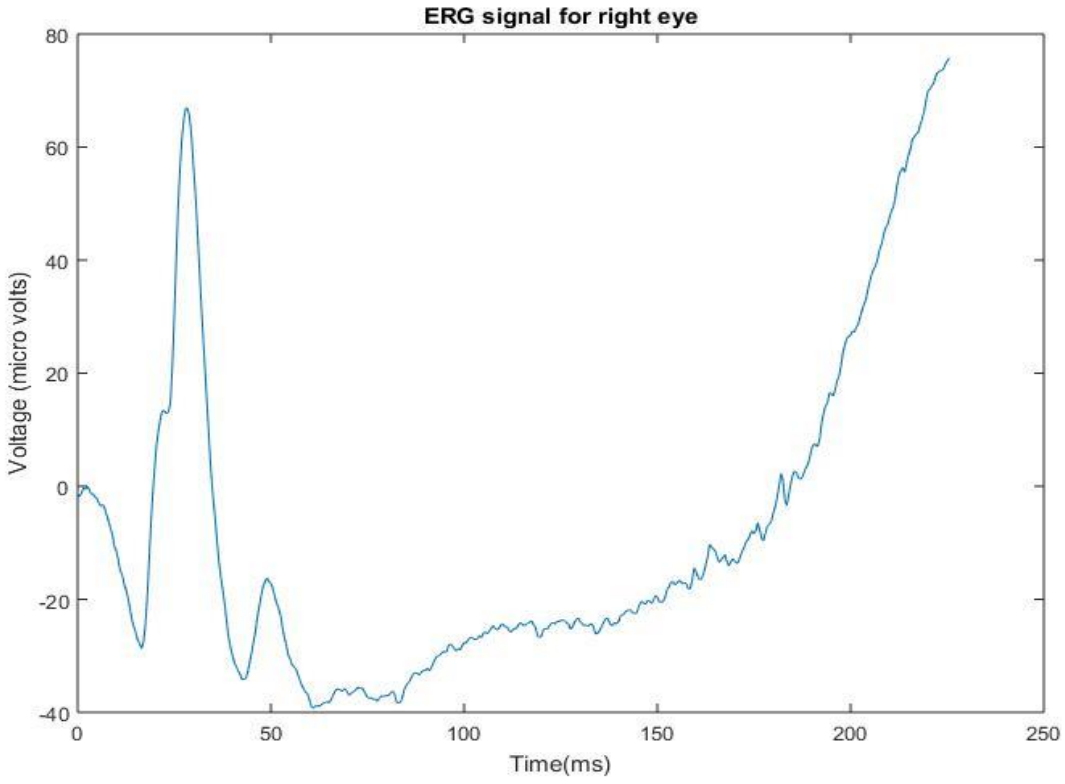

Figure 4: Photopic ERG in Time Domain

The time domain features of a-wave and b-wave of ERG signals is applied by recording the implicit time of the highest point of the wave's peak, as well as the amplitude of the wave's peak. The implicit time of a-wave is 16.5 ms and the highest point at the peak has a voltage value of -28.7 microvolts. B-wave has the highest peak in the ERG where the implicit time is 28 ms which has an amplitude of 66.9 microvolts. The difference in time between the critical points of a-wave and b-wave is 11.5 ms and the difference in amplitude between the two peaks is 95.6 microvolts.

The features of the i-wave and the PhNR in time domain are the implicit time of critical points and the amplitude of their peaks and in the PhNR the signal crosses the baseline from the negative voltage to the positive and that usually marks the tail of the ERG. The implicit time of i-wave is 49 ms and amplitude of the peak at that point is -16.22 microvolts, the difference in voltage between the lowest point of b-wave, which is -34.2 microvolts, and the peak of the i-wave is 17.98 microvolts. The PhNR starts at the tail of the i-wave with an implicit time of 62.5 ms where the lowest value of ERG is located and its value is -38.94 microvolts. The PhNR reaches zero volt for the first time at the time of 181.5 ms, where the signal fluctuates between the negative and positive values before it rises to a high positive value. The following table shows a summary of time domain measurements of the ERG signal.

Following the time domain features, the ERG signal has been run through Fourier transform and the power spectrum of the ERG is shown in figure 5.

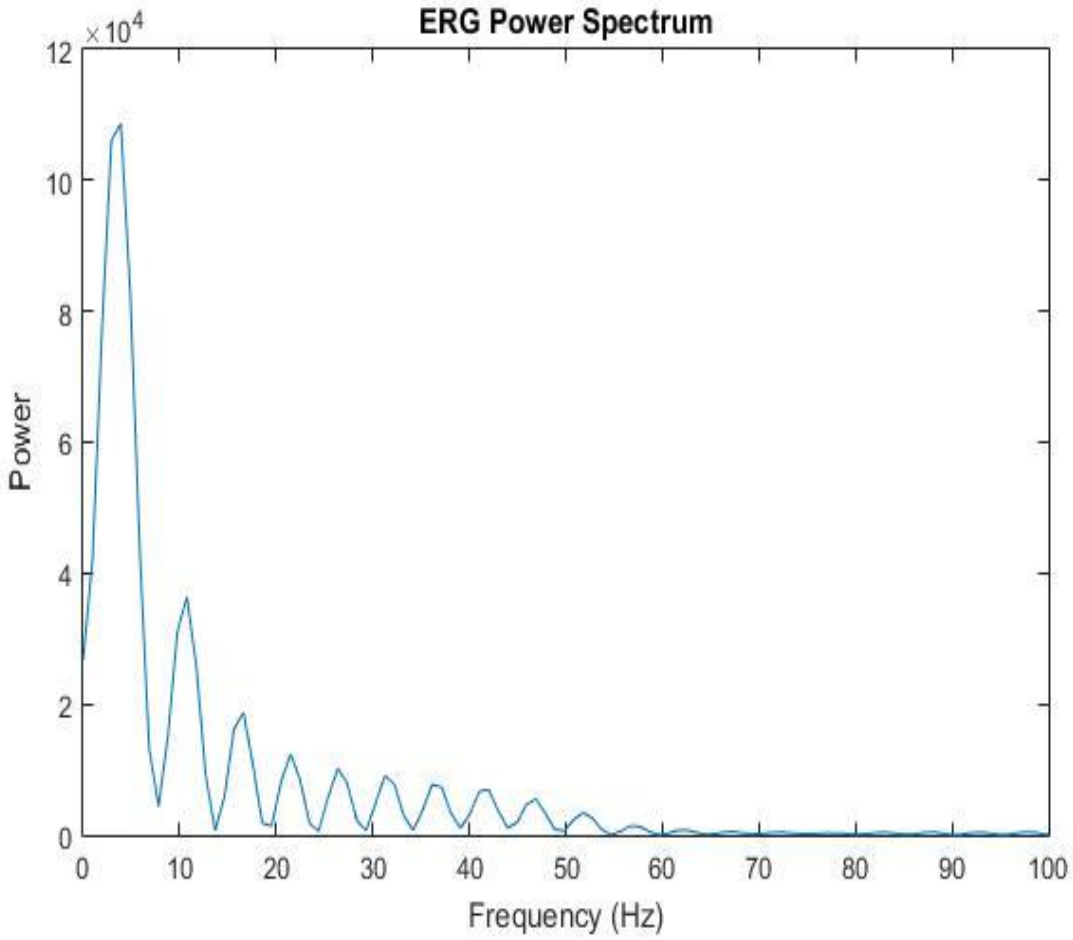

Figure 5: Frequency Domain Plot of the Photopic ERG Response

The ERG power spectrum shows that most of the signal's power is centered on the 4 Hz frequency, the second largest peak and first harmonic is located around 11.9 Hz. Higher frequency components exist within the other few peaks, which are lower in amplitude but are still significant. Oscillatory Potentials (OPs) have higher frequency, these potentials can be decomposed by simply using a high pass filter. However, OPs can also be mistaken for noise since they both share the same power spectrum [22].

The Fourier transform does not show specific details of the signal since most ERG components overlap in the power spectrum. The dominant peaks below 60 Hz contain most of

the ERG power with overlapping components. Further measurements are required to obtain more accurate data, which can be useful in identifying ERG components.

4.3 Short Time Fourier Transform

Since the classical Fourier transform does not offer specific details regarding ERG components, a short time Fourier transform (STFT) is applied to the ERG signal. The STFT is performed in a manner of windowing the original signal into small segments in time domain, each segment is being evaluated individually. In order to increase the accuracy and smoothness of the STFT, each time segment is being overlapped with its neighboring segments. The resulting transform is displayed in a multi-color indexed plot. Figure 6 shows the STFT of the ERG with time presented in x axis and frequency in y axis.

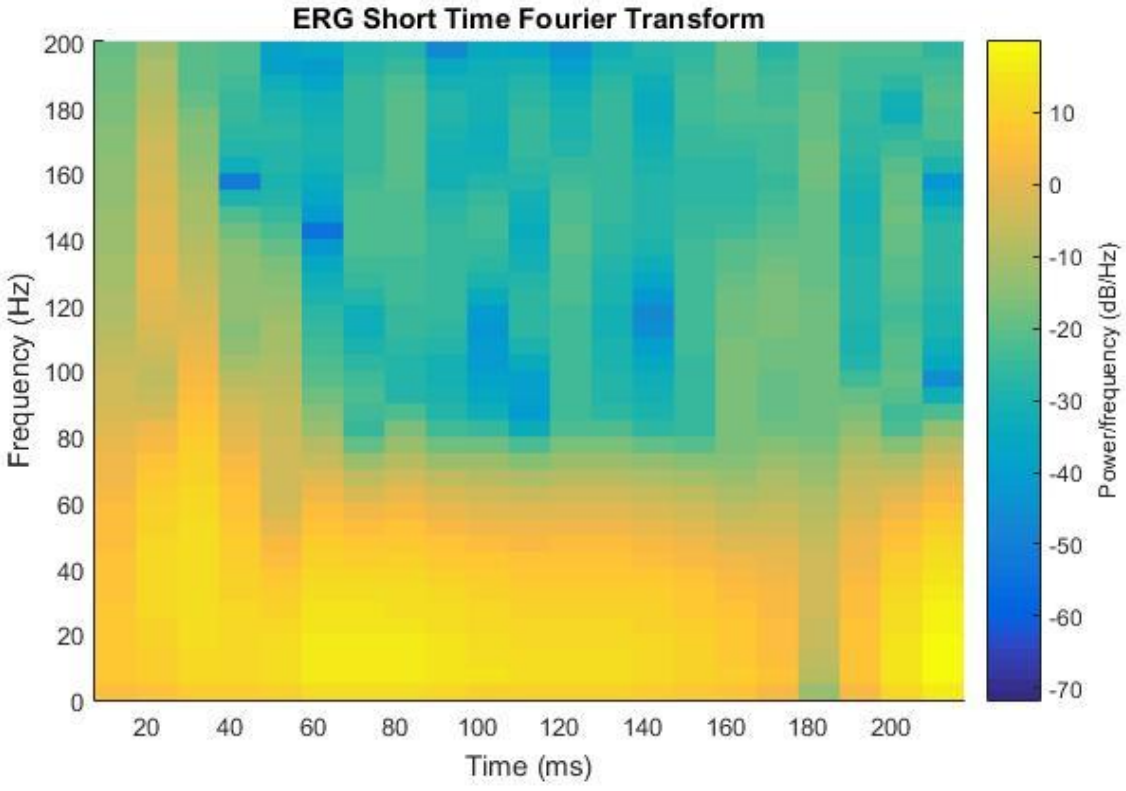

Figure 6: Short Time Fourier Transform of ERG Signal

STFT measurements are usually considered to identify the frequency range of different components of the signal in different times. The negative peak of a-wave is located between 6.5 ms and 19.5 ms, and the highest positive peak of b-wave is located between 20.5 ms and 42.5 ms. The power of a-wave is mostly located in the 0 Hz to 20 Hz band, with a power value of 0 dB/Hz to 6 dB/Hz. Whereas, b-wave has higher power in the band between 10 Hz to 60 Hz with a range of power values between 8 dB/Hz to 15 dB/Hz.

Similarly to a-wave, i-wave has low frequency range in the period between 43ms and 60.5 ms, with frequency range between 3 Hz and 23 Hz. The power band of the i-wave is located around 2 dB/Hz and 5dB/Hz. PhNR has a longer time stamp with almost constant frequency and power factors across the photopic negative response period. In the period of 66 ms to 160 ms, most of PhNR power is located. The frequency fluctuates between 8 Hz and 45 Hz, with a power band between 11 Hz and 18 dB/Hz. A stabilized voltage increase is occurred after the 180 ms point which causes a higher power per frequency value in that period, this increase is connected to the tail of PhNR and can be considered as the tail of the ERG signal.

The measurements of STFT show an approximation of frequency and power bands of the ERG signal in different periods of time, which can be related to the main components of the ERG response. Issues of overlapped bands and lower resolution are present in this measurement, one of the reasons cause these issues is the low sampling frequency rate that made the ERG signal is a 452 point signal with a resolution of 0.5 ms increments.

Another reason for the resolution issues can be considered which is related the nature of ERG response, which makes all components blended in time and frequency domains. Although these issues can alter the STFT measurements, a comprehensive display of the time-frequency representation has been obtained from the application of this tool. Further measurements will be

discussed in this thesis to gain a richer knowledge on the outcomes of each method as well as comparing the results which can be the first step to considering an optimized method of treating ERG responses.

4.4 Continuous Wavelet Transform

Applying the continuous wavelet transform (CWT) to ERG signals has been one of the main methods of analyzing ERG responses [25]. Different mother wavelets are being utilized to serve the signal treating purpose and other DSP analysis. The CWT scaling process is also essential to obtain a realistic outcome and a more specific time-frequency representation. Daubechies (db) mother wavelet is the chosen method for this research, the reason for choosing Daubechies is because it offers acceptable correlation values with ERG signal. The following figure shows the CWT of the ERG signal.

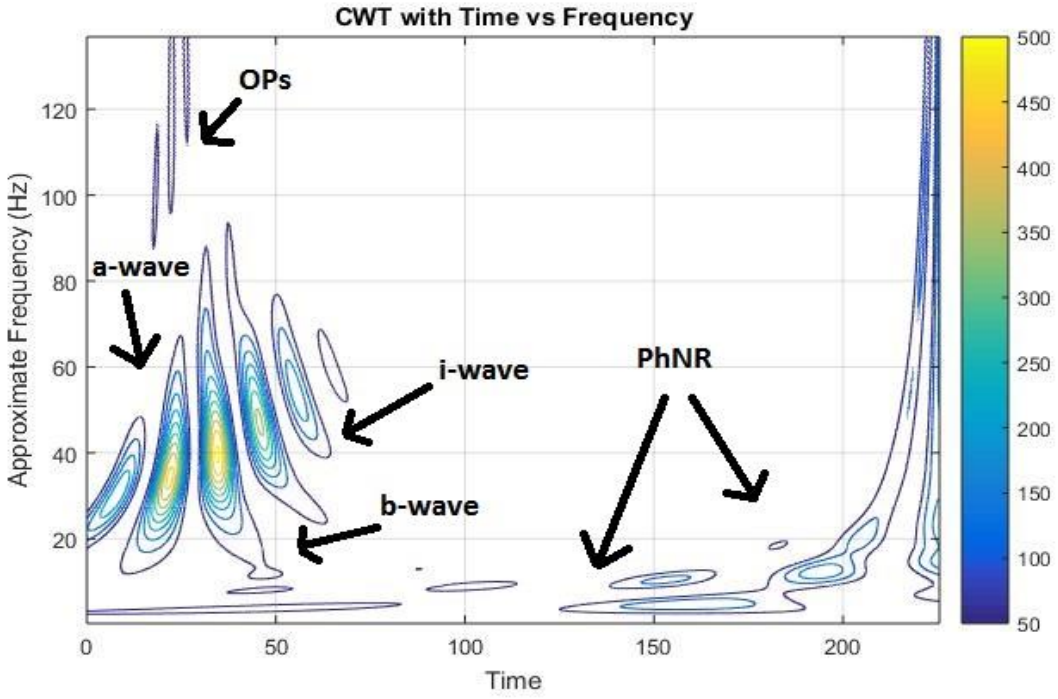

Figure 7: Continuous Wavelet Transform of ERG Signal

Time-frequency analysis can use scales, however it can take longer processing time and power to relate scales to frequency if not initially performed, especially in hardware implementation. Regarding the CWT measurement in figure 7, it is clear that high frequency components only exist before 60 ms. Measurements of frequency and amplitude of ERG response components are to be extracted from the CWT.

A-wave has a low frequency band of 1.7 to 3.9 Hz with amplitude concentrated at 2.9 Hz. Other frequency components exist in the a-wave period, with bands such as 8 Hz to 11 Hz and 23 Hz to 35 Hz. Low amplitude exist in these higher bands, but it is considered essential in the ERG analysis. B-wave has slightly higher frequency band which exists in the range of 2.6 Hz to 5.5 Hz. With higher frequency components existing in b-wave, the frequency band of lower b-wave amplitudes are 6 Hz to 8 Hz and 18 Hz to 54 Hz.

I-wave has a higher frequency band than a-wave, b-wave and PhNR components, reaching 57 Hz in some of its frequency components. With the highest amplitude of i-wave centered between 3 Hz and 5 Hz, other contributions in the frequency bands of 7 Hz to 10 Hz, 11 Hz to 13.4 Hz and 32 Hz to 57 Hz. While the photopic negative response has distributed energies across the frequency band of 2 Hz to 15 Hz, different components exist in PhNR with increasing amplitude with respect to time and also an increase in frequency with respect to time is noticeable.

Oscillatory Potentials (OPs) can be seen in the start of the signal (around 25 ms), with lower amplitude that other ERG components. The frequency band of these OPs measured to be in the band of 70 Hz to140Hz. The OPs are considered the ERG component with the highest frequency band and lowest amplitude. Although, OPs can exist in the entire period of the ERG

signal [34], it is only visible in the early ERG response, i.e. around the b-wave. Figure 11 shows the projection of the Power Spectral Density of the ERG signal against the CWT contour.

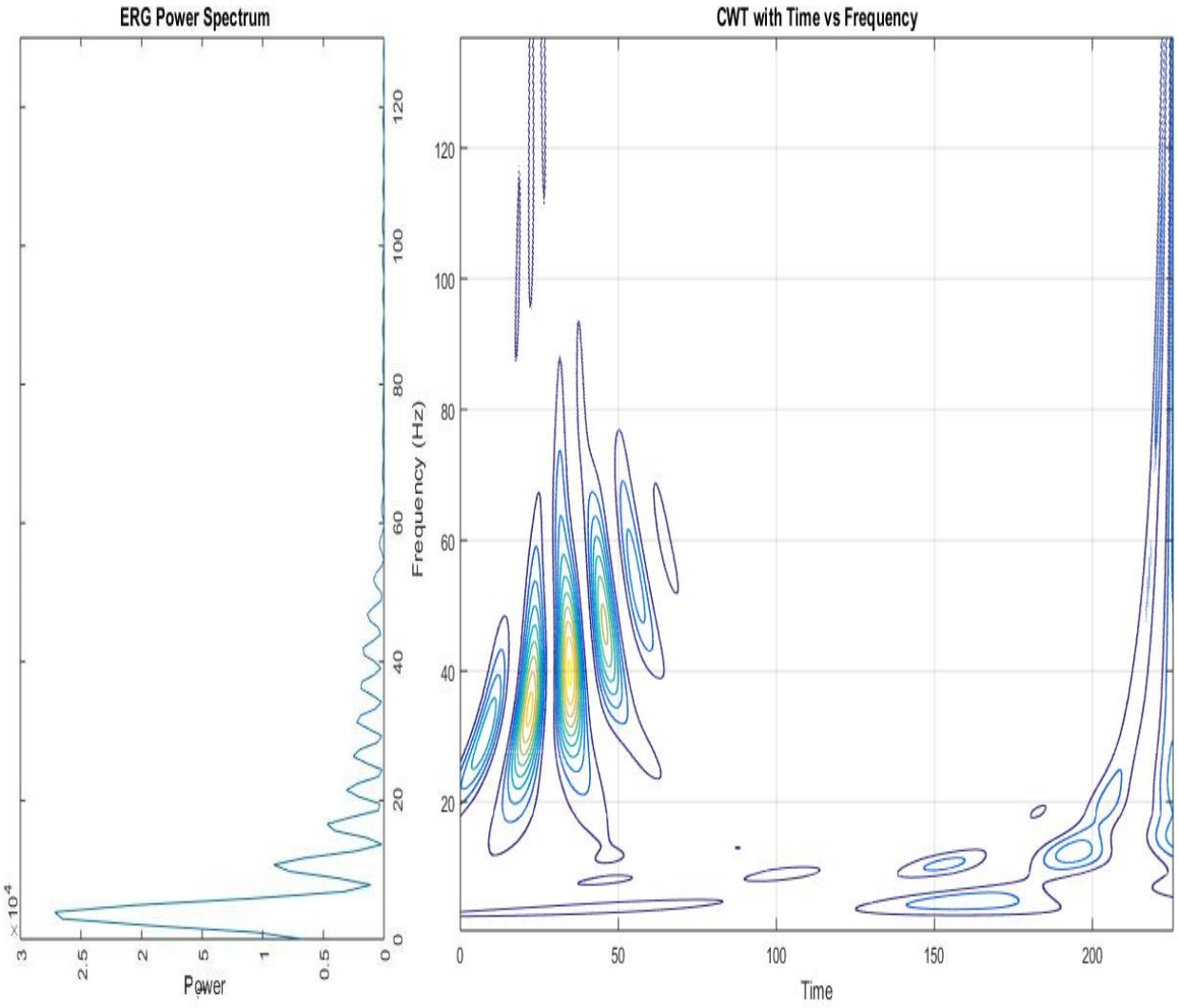

Figure 8: CWT of ERG Signal against FFT Plot

As noticed in Figure 8, the most of the ERG Signal's power is in the low frequency bands, where a-wave, b-wave and PhNR are located, the second highest peak also contains part of a-wave, b-wave and PhNR. I-wave has a higher frequency band and lower spectral power, and OPs have the lowest power in the ERG signal. The CWT is normalized to produce an

accurate energy representation, components, such as OPs, will not be visible if the CWT coefficients are not normalized.

CWT shows a good resolution to the ERG signal, with acceptable and comprehensive time and frequency details. The process of choosing the mother wavelet is critical and can dramatically change the outcome of CWT. Choosing the db10 wavelet has been decided in this research after performing the transform with different wavelets and comparing results and resolutions. Choosing the scales have also been a major concern, different scales produce different type of results and accuracy rates, and more detailed scales lead to high computing power and time being consumed in regard to the performing process. In conclusion, CWT is a reliable method to obtaining ERG information with respect to time and frequency.

4.5 Discrete Wavelet Transform

Applying the transform (DWT) to the ERG signal with the db10 wavelet and a five-level-decomposition, five detail signals and one approximation signal, is the suggested approach in this thesis. The ERG response has been decomposed into five signals with limited frequency band in each resulting signal. Using DWT and Castro's ERG Model, a decomposition process of ERG components is conducted in this section. Castor's ERG model has been used in this part of the thesis to remove a-wave and b-wave components of the signal. The block diagram in figure 9 shows the ERG components decomposition process.

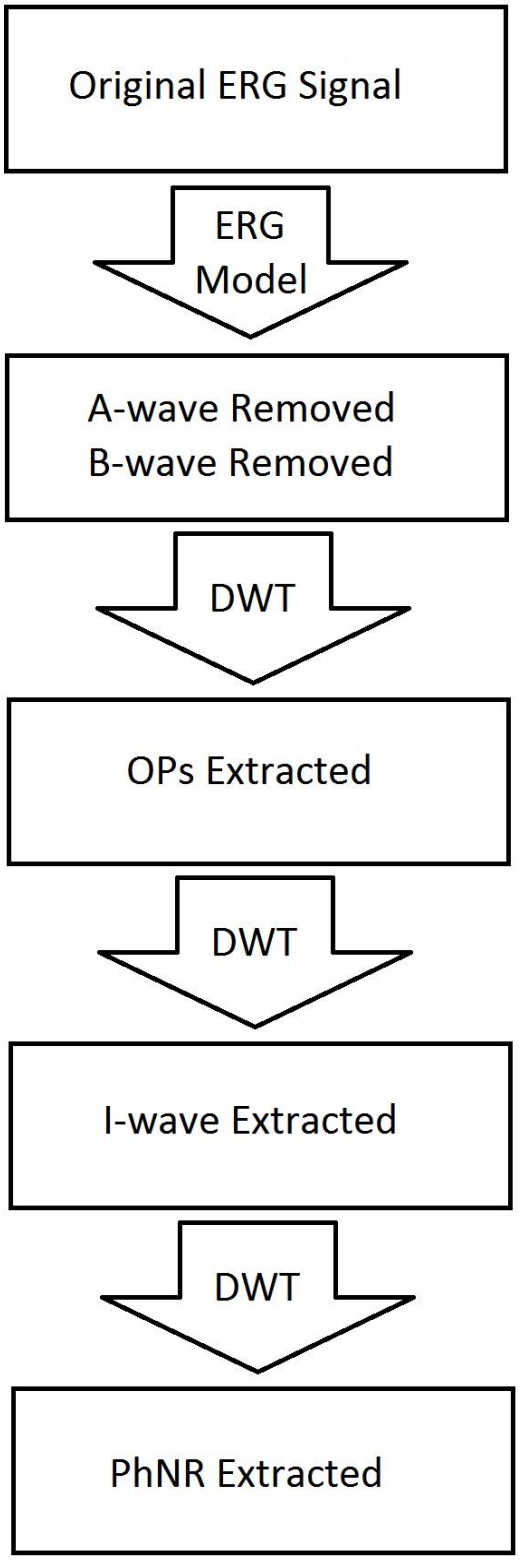

Figure 9: ERG Components Decomposition Process

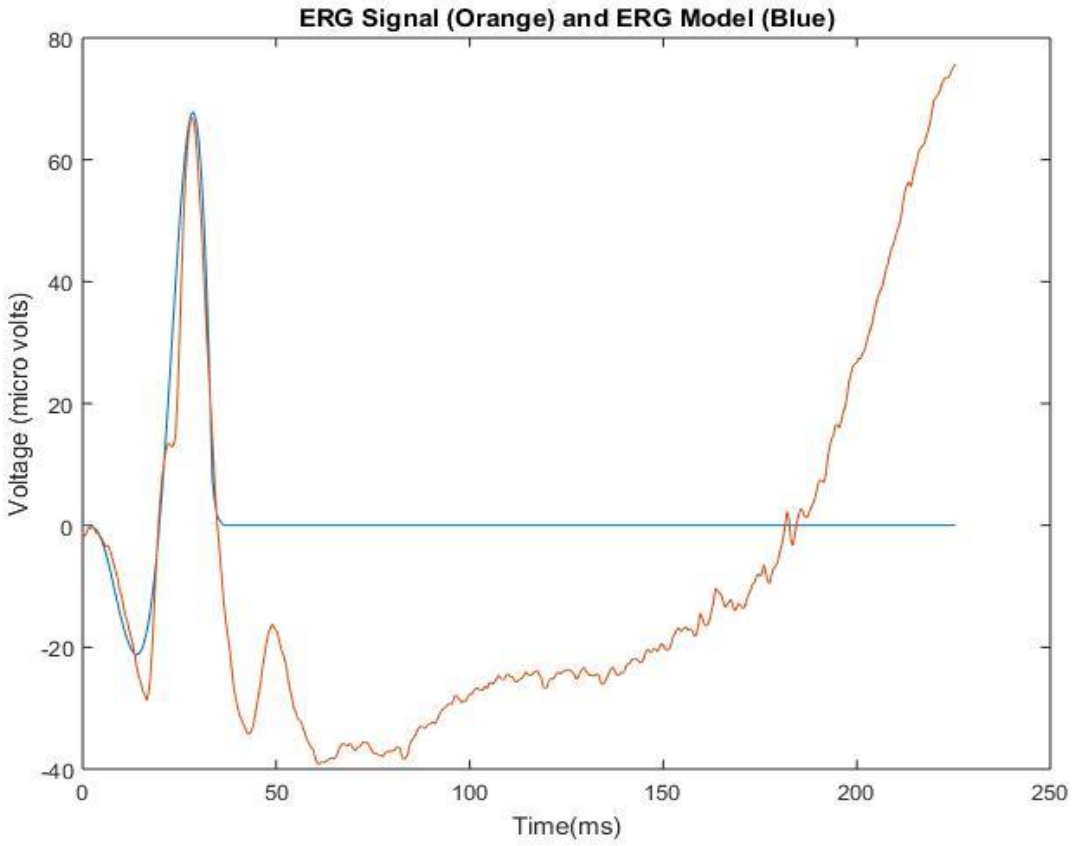

Figure 10: ERG Model Plotted Against Original ERG Signal

As shown in figure 10, The ERG model almost matches the original signal in the early ERG response, an imperfection in the model is noticed in the implicit time of a-wave as well as the peak amplitude. B-wave is matched in both implicit time and peak amplitude. The reason of the difference between the model and the original signal is the presence of OPs and i-wave, other factors could also be considered such as noise and eye movements. The modeled ERG is subtracted from the original signal. Figure 11 shows the resulting signal after the subtraction in time domain and after performing CWT.

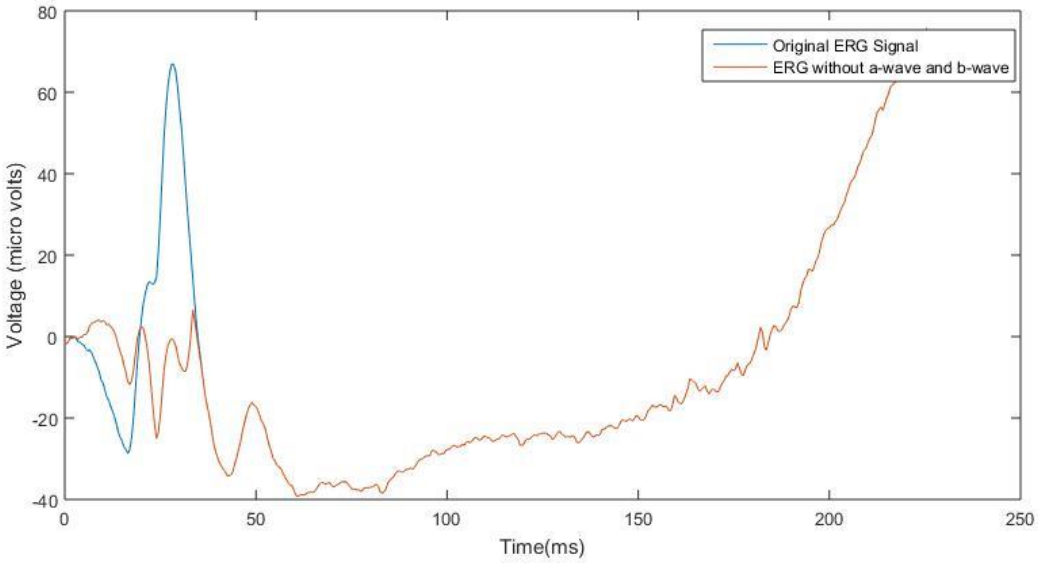

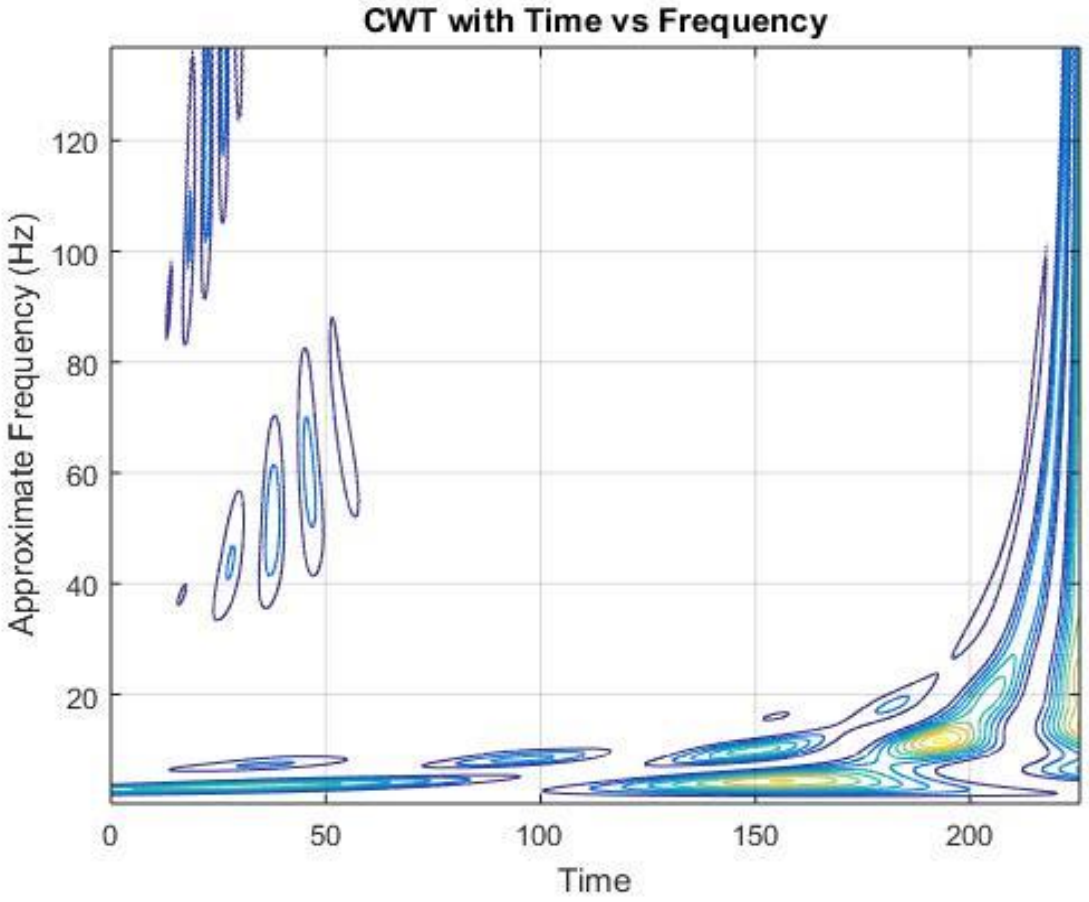

Figure 11: Time Domain and CWT of ERG Signal without a-wave and b-wave

Figure 11 shows the CWT of the ERG with a-wave and b-wave subtracted, and the high energy part of the early ERG response is almost disappeared, which suggests that a-wave and b-wave carried most of the energy of the early response. The obtained signal contains i-wave, PhNR and OPs. The next step of decomposition is to extract OPs using the detail signals obtained from the DWT. The extracted signal in Figure 12 represents the ERG component OPs.

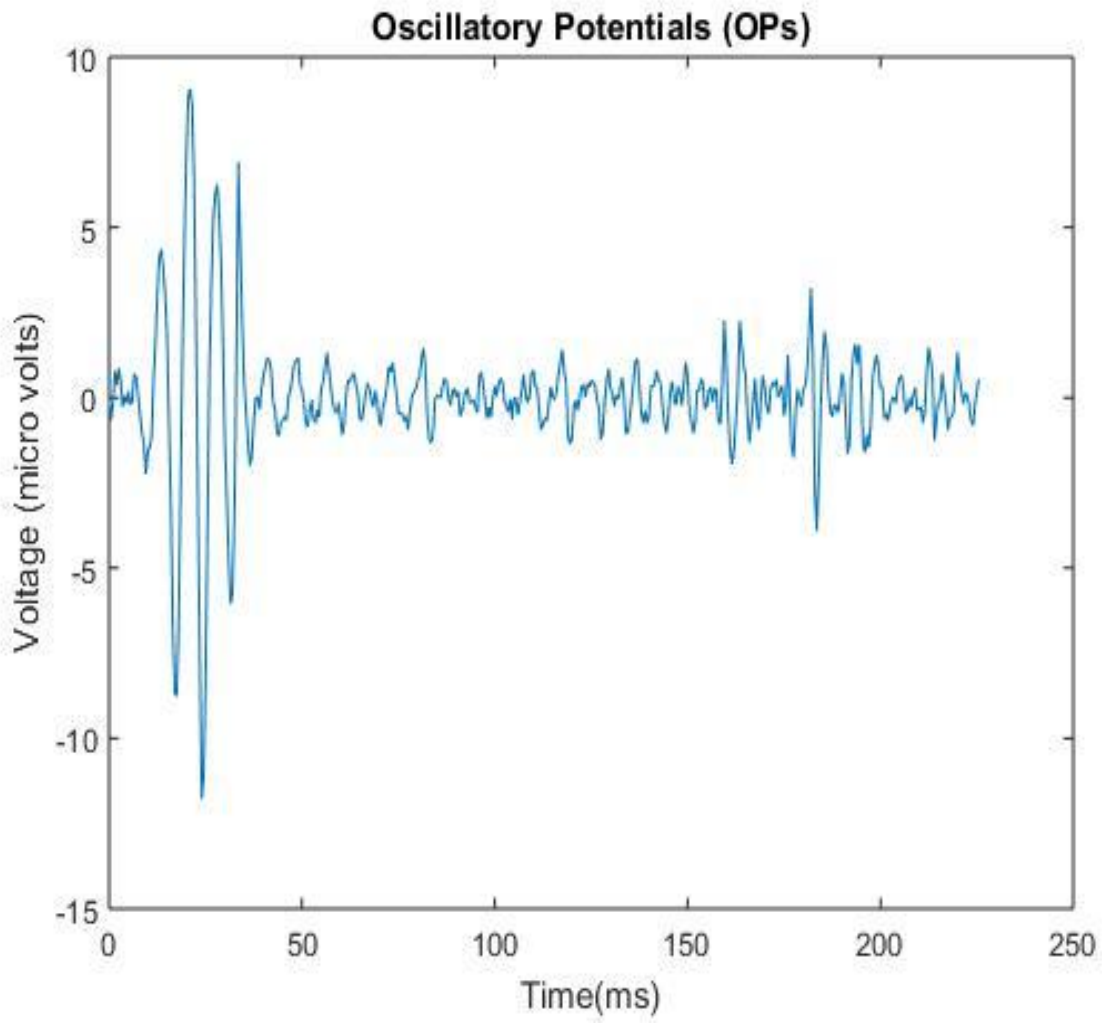

Figure 12: Time Domain Plot of OPs

The high amplitude part of OPs is located in the early response of the signal. Alongside with a-wave and b-wave, OPs are also removed from the ERG signal.

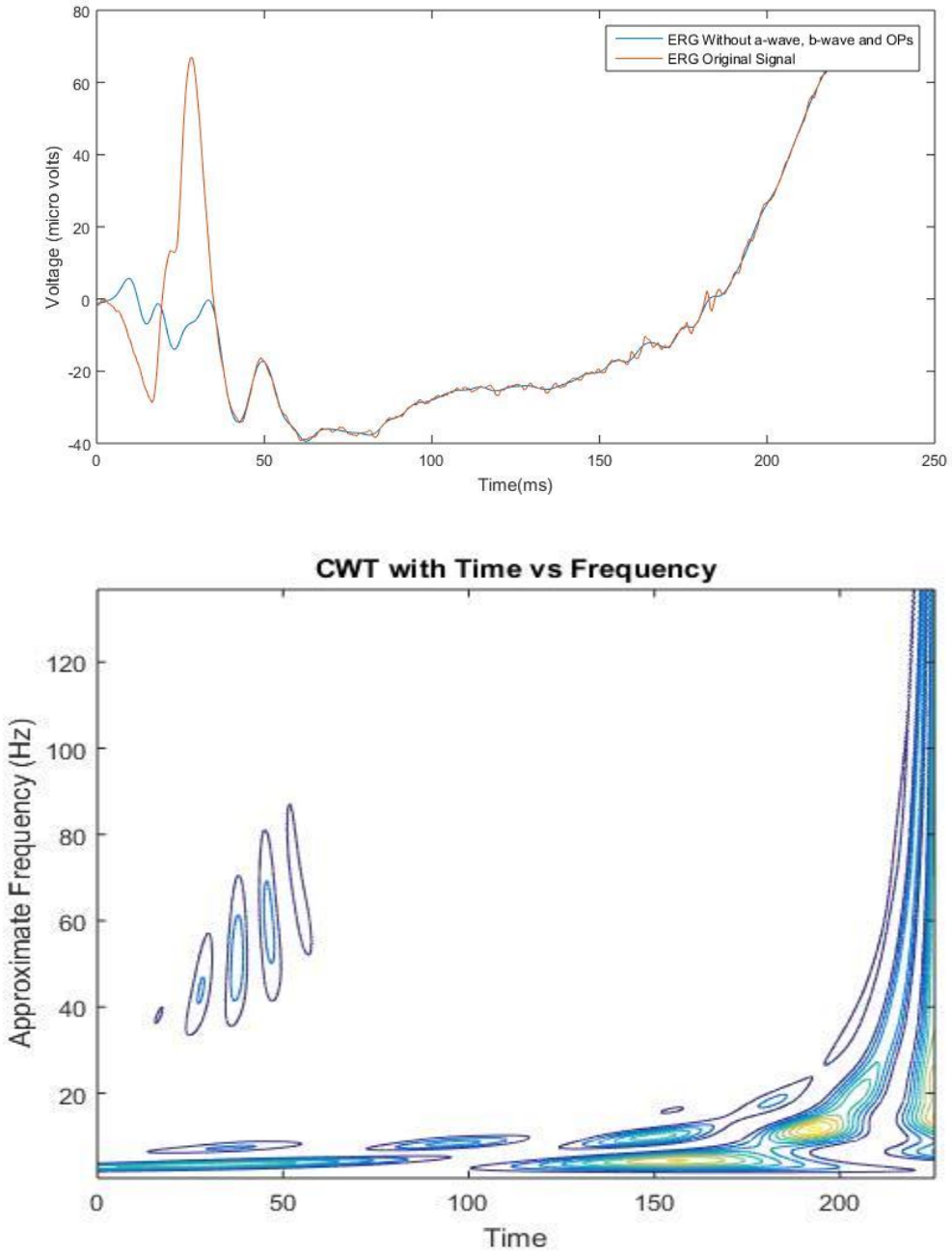

Figure 13: Time Domain and CWT of ERG Signal without a-wave, b-wave and OPs

In figure 13, the resulting signal after removing a-wave, b-wave and OPs is shown in time domain and after applying CWT. In CWT plot, the upper part of the signal is extracted. The part above 80 Hz represents OPs since it is the high frequency component and it has been

extracted. The resulting contour contains i-wave and PhNR. I-wave has a higher frequency band than PhNR, and to separate i-wave and PhNR, DWT is used. The i-wave is isolated by DWT decomposed detail signals. Figure 14 shows the i-wave component.

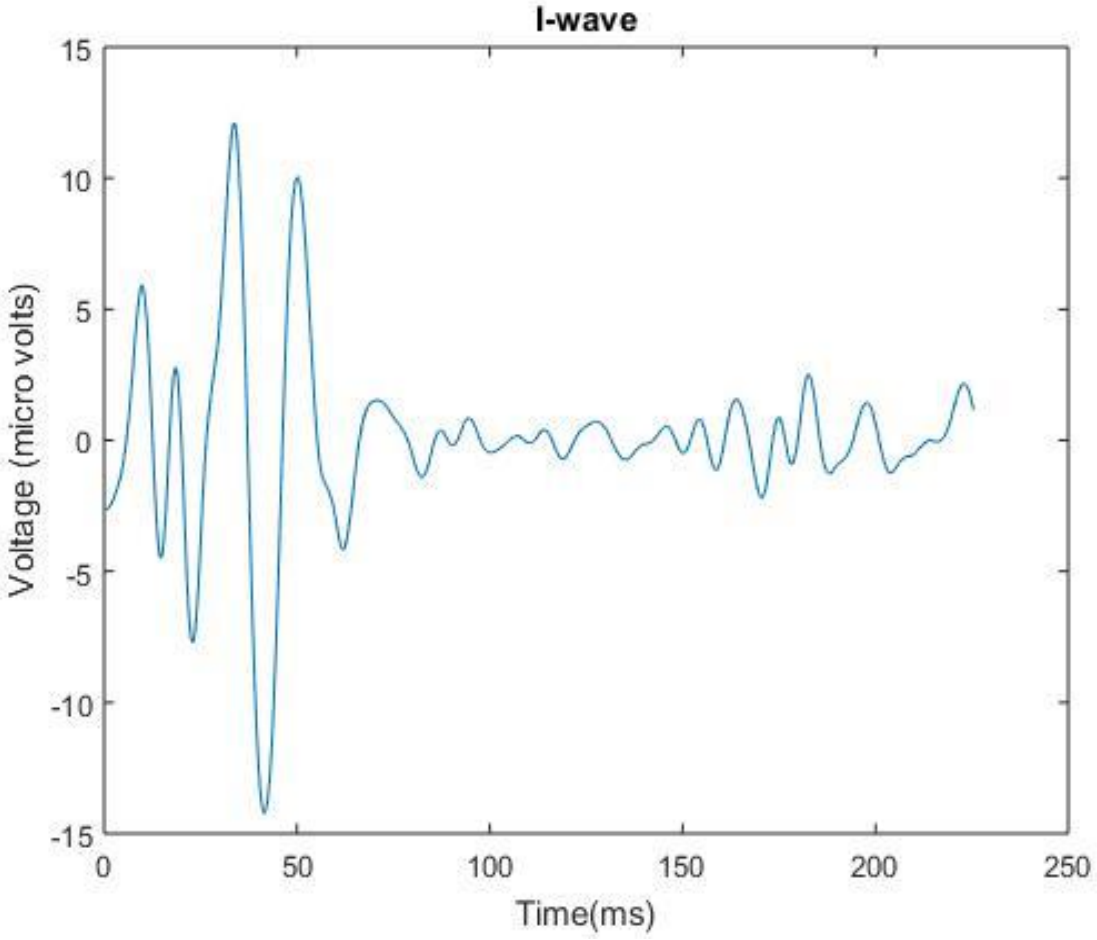

Figure 14: Time Domain of i-wave

Most of i-wave's energy is in the early response of the ERG. The amplitude of i-wave fluctuates between 13 and -15 micro volts. The resultant signal after removing a-wave and b-wave, and after extracting OPs and i-wave will contain PhNR and some leaked contents which are present due to the imperfections of the model and the DWT decomposition.

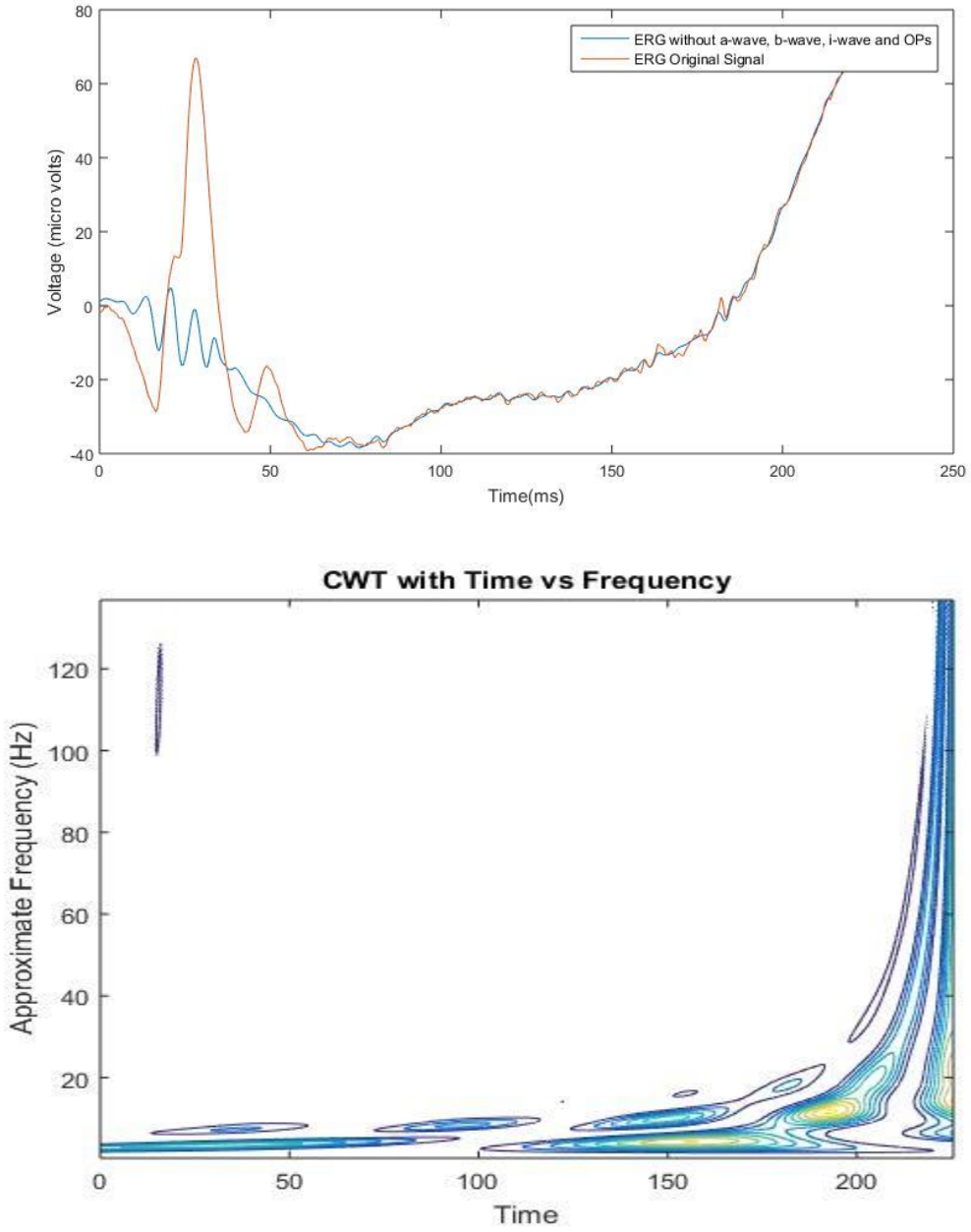

Figure 15: Time Domain and CWT of ERG without a-wave, b-wave i-wave and OPs

The analyzed signal in Figure 15 contains PhNR, which exists in the low frequency band. Some OPs are also visible. PhNR is extracted from the resulting signal using DWT, and Figure 16 shows the obtained PhNR.

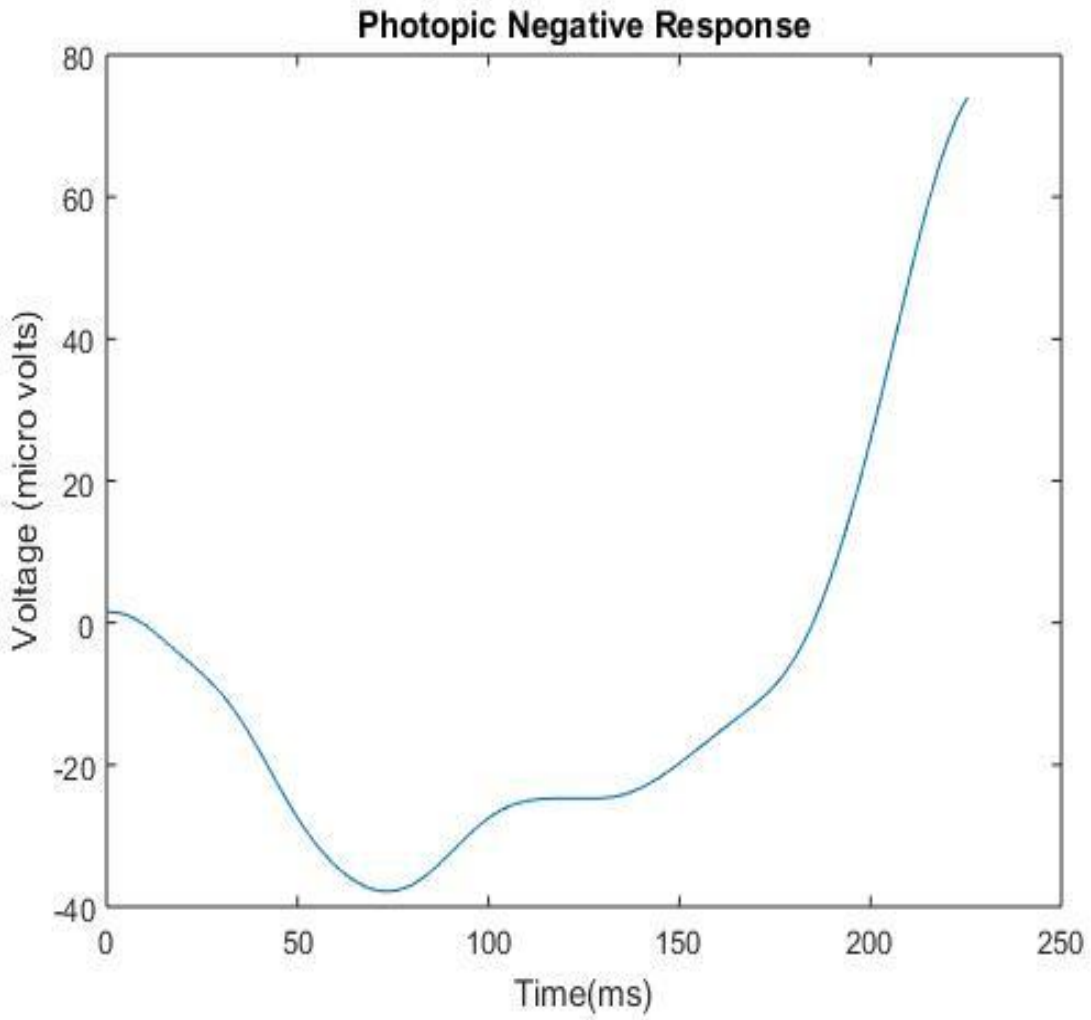

Figure 16: Time Domain Plot of PhNR

As seen in Figure 16, PhNR is a low frequency component which descends from the baseline to its lowest point after the peak of i-wave, it then starts to ascend to reach a higher amplitude. Extracting the PhNR is the last decomposition step and the ERG components have been extracted. Figure 17 shows a superimposed plot of the ERG components.

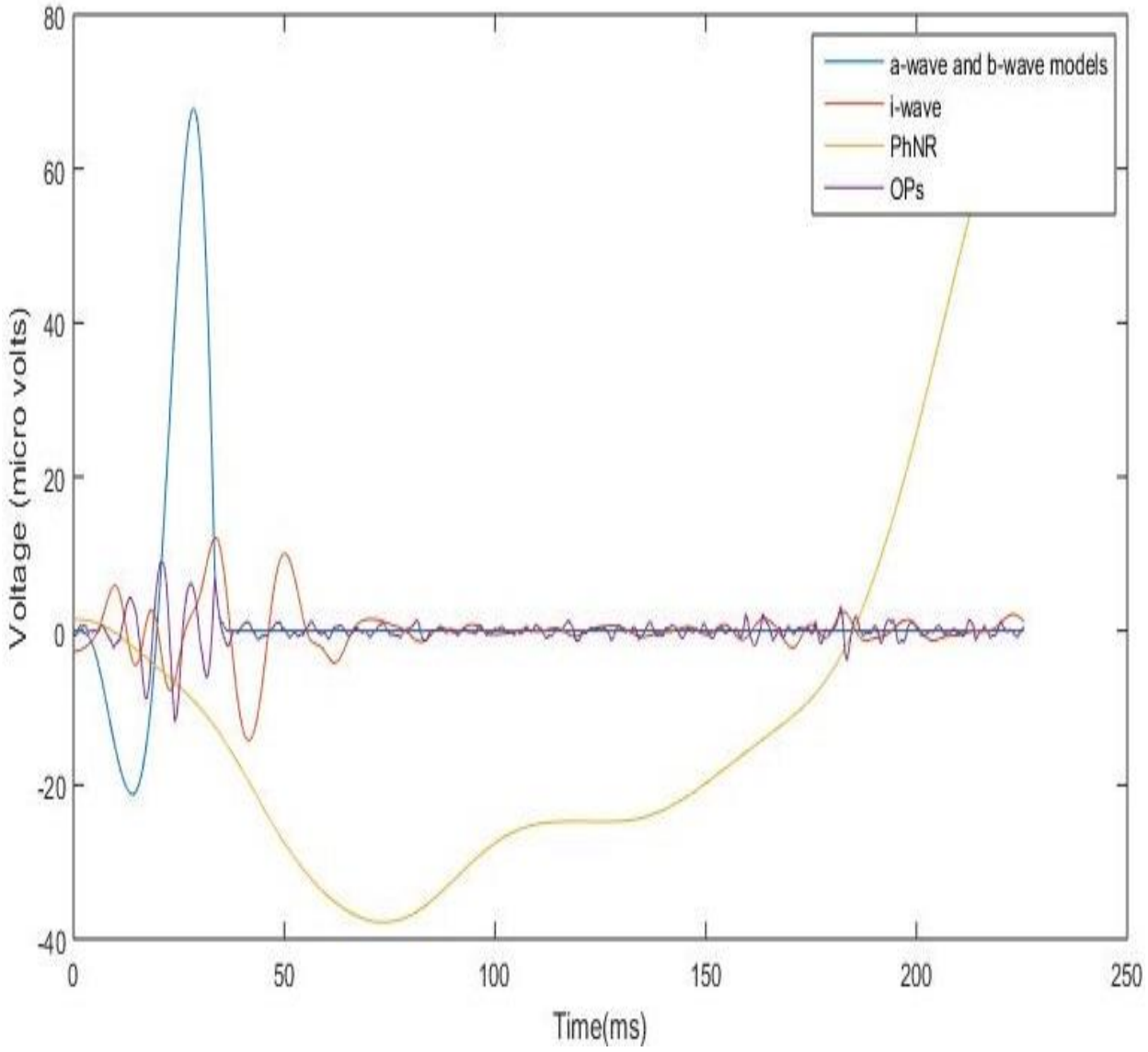

Figure 17: ERG Components Superimposed

Figure 17 shows all extracted ERG components in a superimposed representation. A-wave and b-wave are plotted together since they are modeled. Extracted components are added in figure 18 to reconstruct the ERG signal and plotted against the original ERG.

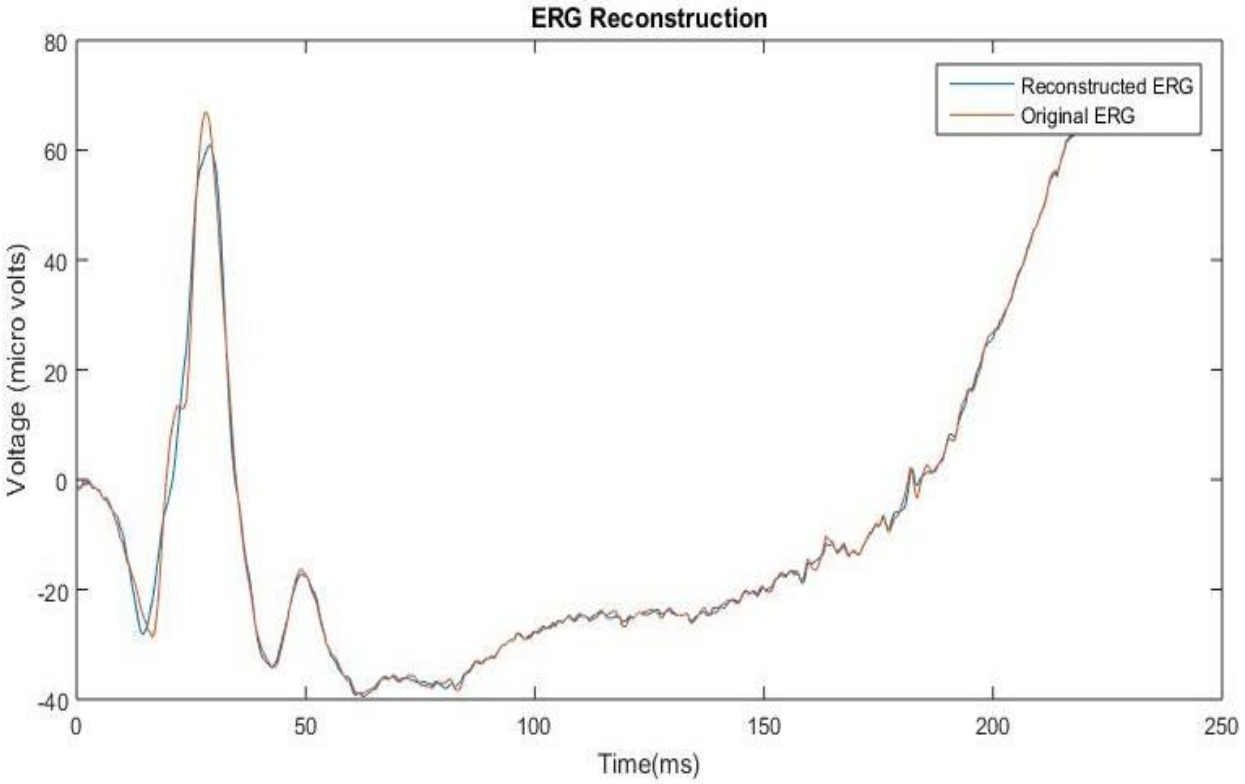

Figure 18: ERG Reconstruction

The plot of the reconstructed signal and the original ERG signal shows small differences which exist mostly in peaks. The shape of the reconstructed signal matches the original one with some noticeable changes in amplitude that have a small margin of difference.

In conclusion, ERG response can be analyzed using a verity of methods which can offer different outcomes depending on the purpose of the analysis. In this chapter different methodologies to observe the photopic response of a human ERG signal were discussed. Decomposition steps have also been performed using discrete wavelet transform and the ERG components have been extracted from the original signal.

CHAPTER 5: DISCUSSION

This chapter will expand the analytical details of the results presented in the previous chapter. A comprehensive analysis will be presented after the examination of obtained features. The photopic ERG response DWT decomposition is also going to be elaborated in this chapter. The optimized approach of examining the ERG response will be discussed in details as well as the findings and contributions.

The analysis of the ERG time domain is based on the implicit time and the peak amplitude of ERG components. The power spectral density analysis using the basic Fourier transform is based on evaluating the dominant peaks in amplitude and their corresponded frequencies. These two analysis methods have been the most common ways to clinically examine the ERG signal and evaluate the retinal condition [33].

The short time Fourier transform shows a simplified time-frequency plot, which provides an indication on which frequency bands the ERG signal lies in. However, it does not offer a specific and detailed time-frequency representation of the signal and the resolution of the plot is relatively low. There are many reasons that make STFT not suitable for ERG examination. Firstly, the ERG signal is a very short signal, which results in low number of segments in the transform. The other reason is that the nature of STFT process requires the user to choose either a low time resolution output, or a low frequency resolution.

Another limitation of STFT is the sharp impulses in the plot caused by applying the transform to the segment borders, which causes an unsmooth frequency representation. In this research, in order to prevent the unsmooth frequency representation, overlapping the transform segments which helps smoothen the output is used. This concludes that the STFT does not offer much useful details in this application.

The continuous wavelet transform relates the time axis of the ERG signal to scaled and shifted wavelets that are directly related to frequencies. This transform offers a very detailed time to scale plot which can be approximated to a time-frequency plot that represent the ERG response frequency bands in a detailed manner. CWT is mainly dependent on the mother wavelet chosen to be convolved across the ERG signal; the chosen wavelet (Daubechies) has been proved to be a suitable wavelet with balanced outcome and less unused coefficients. The scales value have been chosen based on a binary system that can give a high resolution plot while performing minimal number of dilations. The CWT algorithms developed in this thesis proved to be a good representation of a time-frequency ERG response. This transform has a limitation in the number of processing steps performed in order to obtain the coefficients.

CWT may have an affected output due to the cone of influence. The CWT, convolution based, algorithm treats the signal as a non-periodic input with all other values in the plane assumed to be zeros. The cone of influence does not occur in the start of the ERG since the start value of the signal is almost zero. The effect is carried out at the end of the ERG signal where the voltage is at the highest point.

The cone of influence causes the CWT to produce coefficients in low scales (high frequency). This can be considered a disadvantage since it can alter the overall analysis, especially the PhNR analysis. The ERG signal is tested in the period 0 ms to170 ms, where the

PhNR ascends from the lowest point in amplitude to zero. A comparison of CWT of the full ERG signal and the shortened signal is discussed. In Figure 19, the CWT applied to the full ERG signal (left) shows a high amplitude at the end of the ERG signal towards the lower scales (high frequency), while the shortened ERG does not show any change in scales at the end of the signal.

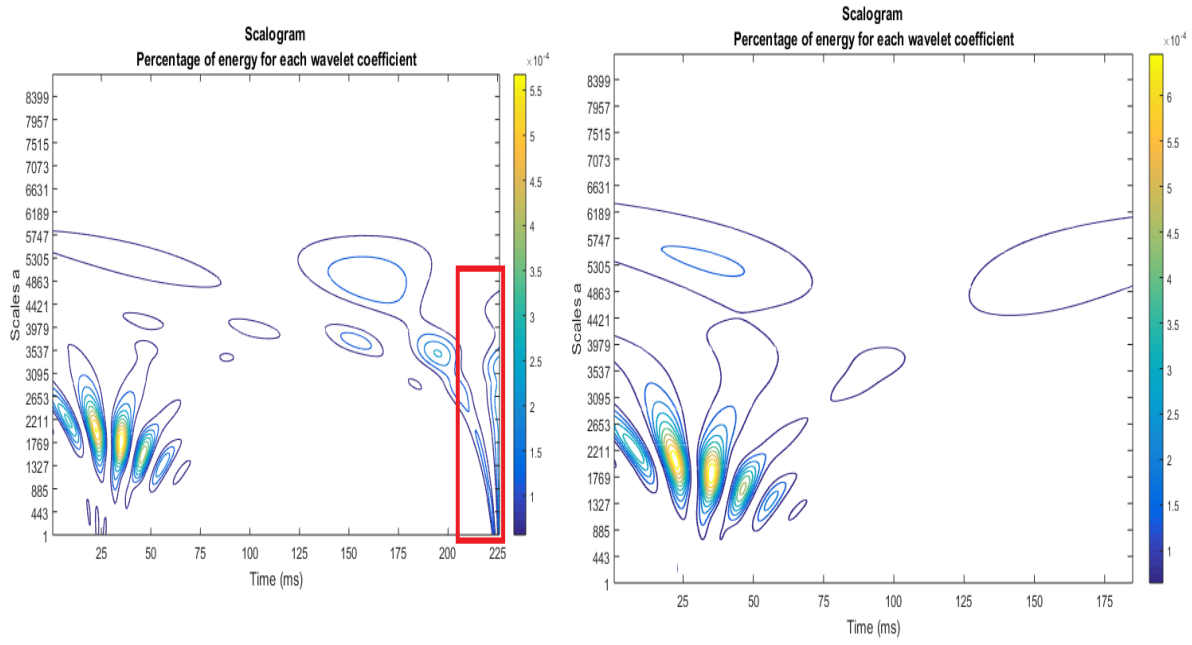

Figure 19: The Effect of Cone of Influence in CWT

This leakage shown in figure 19 (left) is caused by the cone of influence effect, which occurs if the final sample of the ERG signal has a high amplitude, and the CWT considers the value after the last sample to be zero, which forms a sudden change in voltage which is considered as a high frequency value.

DWT carried out in this thesis was also based on the Daubechies mother wavelet. The outcome of the transform is a visual representation of time-frequency analysis, with an amplitude

identified in the colored index. The visual time-frequency representation of the DWT is limited with less resolution than CWT, which makes the DWT not suitable for visual analysis. However, the DWT offers a set of decomposed signals due to the filtering process of DWT. Each decomposed signal has its unique frequency band. The addition of all decomposed signals will result in a reconstructed ERG signal which matches the original ERG response. These decomposed signals can be analyzed individually to study the behavior of the ERG signal in time domain in each decomposed signal.

After using Castor's Model, the process of extraction of other ERG components was conducted. The model does not match the a-wave and b-wave exactly, which means that the model was either approximated or the other ERG signals have affected the early response of ERG. OPs were the first to be extracted since they have the highest frequency band. I-wave and PhNR have been extracted from the resulting signal. The extracted components have been used to reconstruct the ERG signal, with some minor differences in the peaks and other parts of the signal.

In conclusion, this chapter discussed the advantages and disadvantages of each technique used to analyze the ERG signal, CWT is considered the most suitable approach for visualizing the time-frequency representation. In comparison, DWT offers more details on decomposed signals which can be analyzed individually in time domain. Some limitations are noticed in the applied techniques, such as the ambiguous power spectra in FFT, the low resolution in STFT, the matter of choosing a suitable wavelet and the effect of cone of influence in CWT and finally the reduced sampling rate in DWT.

CHAPTER 6: CONCLUSION

In this research, various techniques of signal processing have been investigated in detail to analyze the ERG signal. The origin of the ERG signal has been described. The medical advantage of analyzing the ERG test has also been emphasized. Different types of ERG signals have been introduced with details regarding obtaining each one. ERG data collection process has also been identified. Different DSP methods were performed on the ERG signal. The results of each method have been described and compared in detail. In addition, the research concluded with a discussion of the obtained results showing the advantages and some limitations.

DSP techniques which are utilized in this thesis included STFT, CWT and DWT. Analyzed data of each method was presented and summarized. A comparison of the applied techniques showed that some techniques are more suitable than others are. Configurations set to each techniques are also proven to be essential. And finally, the advantages and disadvantages of each technique has been identified.

Further research can be conducted in the ERG signal processing field, where other mother wavelets can be used as well as other Daubechies wavelet levels. The ERG noise is also an important area of study and a process of denoising the signal, which can differ between high frequency ERG components, and signal noise is needed. Finally, further research is also suggested for developing efficient DSP algorithms of ERG signal analysis which can be implemented in hardware, preferably FPGAs.

Different DSP approaches are also needed for a wider exploration in ERG signals. Statistical approaches should be considered in analyzing ERG signals. Various statistical tools and algorithms should be used for ERG signal analysis.

The data collection process is one of the important areas to explore. Most of current methods provide a signal that contains various components originating in different parts of the eye. An improved data collection process can provide a more detailed response which can help identify ERG components accurately. The sampling rate of the data should also be improved. ERG responses are very short and most of the essential components are present in the first part of the response (first 50 milliseconds). A better sampling rate will produce a better resolution which is needed to apply a wider range of DSP techniques.

There has not been any available database that offers ERG signals of different types. Many bio-medical applications have been improved and widely explored due to the availability of diverse databases such as ECG signals. Databases for ERG responses should be an essential step to conduct more detailed studies and obtain improved results.

The lack of ERG models is a noticeable challenge. Since there are only few models for ERG signals, they only focus on the generalized components such as a-wave and b-wave. A configurable model with specific details regarding the type of ERG response, subject's gender and age, and light intensity is needed. The availability of ERG models can help analyze and decompose ERG signals with more clarity and ease, it can also help implement automated processes for ERG analysis.

Finally, a promising approach has been developed in this thesis to help standardize ERG components and expand the analysis capabilities.

REFERENCES

[1] Ala-Laurila P, Cornwall MC, Crouch RK, Kono M. The action of 11-cis-retinol on cone opsins and intact cone photoreceptors. J Biol Chem. 2009;284:16492-16500.

[2] Arden GB, Barrada A, Kelsy JH. New clinical test of retinal function based on the standing potential of the eye. Br J Ophthalmol. 1962;46:449–467.

[3] Arden, GB, Friedman, A. and Kolb. H. (1962) Anticipation of chloroquine retinopathy. The Lancet, June 2, pp 1164-1165.

[4] Boughman JA, Fishman GA. A genetic analysis of retinitis pigmentosa. Br J Ophthalmol. 1983;67:449–454.

[5] Creel DJ, Crandall AS, Ziter FA. Identification of minimal expression of myotonic dystrophy using electroretinography. Electroencephalogr Clin Neurophysiol.1985;61:229–235.

[6] Creel DJ, Wang JM, Wong KC. Transient blindness associated with transurethral resection of the prostate. Arch Ophthalmol. 1987;105:1537–1539.

[7] Cobb WA, Morton HB. A new component of the human electroretinogram. J Physiol. 1954;123:36P–37P.

[8] Costedoat-Chalumeau N, Ingster-Moati I, Leroux G, et al. Critical review of the new recommendations on screening for hydroxychloroquine retinopathy [in French]. Rev Med Interne. 2012;33(5):265-267.

[9] Granit R. The components of the retinal action potential in mammals and their relation to the discharge in the optic nerve. J Physiol. 1933;77:207–239.

[10] Hartzell HC, Zhiqiang Q, Kuai Y, Xiao Q, and Chien LT (2008) Molecular physiology of bestrophins: multifunctional membrane proteins linked to Best Disease and other retinopathies. Physiol. Rev. 88: 639-672.

[11] Rosolen SG, Rigaudiere F, LeGargasson JF, Chalier C, Rufiange M, Racine J, Joly S, Lachapelle P (2004) Comparing the photopic ERG.

[12] i-wave in different species. Vet Viswanathan S, Frishman LJ, Robson JG, Walters JW (2001) The photopic negative response of the flash electroretinogram in primary open angle glaucoma. Invest Ophthalmol Vis Sci 42(2):514–522.

[13] Rangaswamy NV, Frishman LJ, Dorotheo EU, Schiffman JS, Bahrani HM, Tang RA (2004) Photopic ERGs in patients with optic neuropathies: comparison with primate ERGs after pharmacologic blockade of inner retina. Invest Ophthalmol Vis Sci 45(10):38273837.doi:10.1167/iovs.04-045845/10/3827[pii].

[14] Hindawi Publishing Corporation Journal of Ophthalmology Volume 2012, Article ID 397178, doi:10.1155/2012/397178.

[15] K. Gadhoumi, J. Lina, and J. Gotman, "Discriminating preictal and interictal states in patients with temporal lobe epilepsy using wavelet analysis of intracerebral EEG," *Clinical Neurophysiology*, vol. 123, no. 10, pp. 1906–1916, 2012.

[16] P. S. Addison, "Wavelet transforms and the ECG: a review," *Physiological Measurement*, vol. 26, no. 5, pp. R155–R199, 2005.

[17] A. Phinyomark, C. Limsakul, and P. Phukpattaranont, "Application of wavelet analysis in EMG feature extraction for pattern classification," *Measurement Science Review*, vol. 11, no. 2, pp. 45–52, 2011.

[18] J.D. Forte,B.V.Bui, andA. J. Vingrys, "Wavelet analysis reveals dynamics of rat oscillatory potentials," *Journal of Neuroscience Methods*, vol. 169, no. 1, pp. 191–200, 2008.

[19] J. M. Miguel-Jim´enez, L. Boquete, S. Ortega, J. M. Rodr´ıguez- Ascariz, and R. Blanco, "Glaucoma detection by wavelet-based analysis of the global flash multifocal electroretinogram," *Medical Engineering and Physics*, vol. 32, no. 6, pp. 617–622, 2010.

[20] Machida S, Gotoh Y, Toba Y, Ohtaki A, Kaneko M, Kurosaka D,Correlation between Photopic Negative Response and Retinal Nerve Fiber Layer Thickness and Optic Disc Topography in Glaucomatous Eyes Investigative Ophthalmology & Visual Science, May 2008, Vol. 49, No. 5.

[21] McAnany JJ, Nolan PR Changes in the harmonic components of the flicker electroretinogram during light adaptation, Doc Ophthalmol. 2014 Aug;129(1):1-8. doi: 10.1007/s10633-014-9437-y. Epub 2014 May 1.

[22] McCulloch DL, Marmor MF, Brigell MG, Hamilton R, Holder GE, Tzekov R, Bach M ISCEV Standard for full-field clinical electroretinography (2015 update). Doc Ophthalmol 130:1–12

[23] Miller RF, Dowling JE, Intracellular responses of the Muller (glial) cells of mudpuppy retina: their relation to b-wave of the Electroretinogram J Neurophysiol 1970;33;323-341

[24] Moss HE., Park JC, McAnany JJ, The Photopic Negative Response in Idiopathic Intracranial Hypertension, Invest Ophthalmol Vis Sci. 2015;56:3709–3714. DOI:10.1167/ iovs.15-16586

[25] Nair SS., Joseph KP., Wavelet based electroretinographic signal analysis for diagnosis, Biomedical Signal Processing and Control 9 (2014) 37– 44

[26] Nakazawa T1, Takahashi H, Nishijima K, Shimura M, Fuse N, Tamai M, Hafezi-Moghadam A, Nishida K. Pitavastatin prevents NMDA-induced retinal ganglion cell death by suppressing leukocyte recruitment. J Neurochem. 2007 Feb;100(4):1018-31.

[27] Palmowski AM, Sutter EE, Bearse MA, Jr., Fung W. Mapping of retinal function in diabetic retinopathy using the multifocal electroretinogram. Investigative ophthalmology & visual science. 1997;38(12):2586-96.

[28] Radhakrishnan K, Thacker AK, Bohlaga NH, et al. Epidemiology of idiopathic intracranial hypertension: a prospective and case-control study. J Neurol Sci. 1993; 116:18–28.

[29] Radhakrishnan K, Ahlskog JE, Cross SA, et al. Idiopathic intracranial hypertension (pseudotumor cerebri) descriptive epidemiology in Rochester, Minn, 1976 to 1990. Arch Neurol. 1993;50:78–80.

[30] Rangaswamy NV., Shirato S., Kaneko M., Digby BI., Robson JG. and Frishman LJ., Effects of Spectral Characteristics of Ganzfeld Stimuli on the Photopic Negative Response (PhNR) of the ERG, Invest Ophthalmol Vis Sci. 2007 October ; 48(10): 4818–4828.

[31] Rioul O, Vetterli M, Wavelets and signal processing, IEEE SP Magazine, 1053-5888/91/1000-0014, 1991

[32] Robson JG, Saszik SM, Ahmed J, Frishman LJ, Rod and cone contributions to the a-wave of the Electroretinogram of dark adapted macaque, J. Physiol (Lond)2003;547;509-530

[33] Robson JG, Frishman LJ, Response linearity and Kinetics of the cat retina: The bipolar-cell component of the dark-adapted Electroretinogram, Vis Neurosci, 1995,12;237-850

[34] Rowe FJ, Sarkies NJ. Assessment of visual function in idiopathic intracranial hypertension: a prospective study. Eye.1998; 12:111–118

[35] Mallat SG, "Theory formultiresolution signal decomposition: the wavelet representation," IEEE Transactions on Pattern Analysis and Machine Intelligence, vol. 11, no. 7, pp. 674–693, 1989.

[36] Schiff SJ, Aldroubi A, Unser M, Sato S, Fast wavelet transformation of EEG, Electroencephalography and clinical Neurophysiology, 91 (1994) 442-455

[37] Sieving PA, Arnold EB, Jamison J, Liepa A, Coats C, Submicrovolt Flicker Electroretinogram: Cycle-by-Cycle Recording of Multiple Harmonics with Statistical Estimation of Measurement Uncertainty, Investigative Ophthalmology & Visual Science, July 1998, Vol. 39, No. 8

[38] Sieving PA, Murayama K, Naarendorp F, Push-pull model of the primate photopic electroretinogram: A role for hyperpolarizing neurons in shaping the b-wave, Vis Neurosci, 1994;11;519-532

[39] Stockton RA, Slaughter MM, The b-wave of the elctroretinogram: A reflection of ON bipolar cell activity. J Gen Physiol 1989;93;101-122

[40] Tomita T, Studies on the intraretinal action potential: Relation between the localization of micropipette in the retina and the shape of the intraretinal action potential. Jpn J Physiol1950,1;110-117

[41] Tomita T, Funaishi A, Studies on intraretinal action potential with low resistance microelectrodes,1952, 15;75-84

[42] Torren KVD., Groeneweg G., Lith GV. Measuring Oscillatory Potentials: Fourier Analysis, Documenta Ophthalmologica 69; 153-159 (1988)

[43] Modeling Of Electroretinogram *And* Its Relation To Stimulus Light Intensity, Juan J. Castro Andrew U. Meyer Edward I. Haup, Biophysical and Biochemical Measurements 8.3-1

APPENDIX A: LIST OF ABBREVIATIONS

ERG	Electroretinogram
PhNR	Photopic Negative Response
DSP	Digital Signal Processing
OP	Oscillatory Potentials
RGC	Retinal Ganglion Cells
CWT	Continuous Wavelet Transform
DWT	Discrete Wavelet Transform

APPENDIX B: MATLAB CODES

B.1 MATLAB Code for Time Domain Representation

```
clc;
clear all;
close all;

%------------------------------------------------ ERG Signal

s=xlsread(‘RT_OD&OS_RF_WB_042215.xls'); % ERG Signal excel file


t=[-30:0.5:225.5];

t_ms=t./1000;

f=2000;  %  sampling frequency of 2000 Hz

plot(t,s);

title('ERG signal for right eye');

xlabel('Time(ms)');

ylabel('Voltage (micro volts)');
```

B.2 MATLAB Code for Time Frequency Representation

```
clc;
clear all;
close all;

%------------------------------------------------ ERG Signal

s=xlsread(‘RT_OD&OS_RF_WB_042215.xls'); % ERG Signal excel file


t=[-30:0.5:225.5];
```

```
fs=2000;

m = length(s);          % Window length

n = 2048;  % Transform length

y = fft(s,n);           % DFT

f = [ 0 :1000/1023.5 : 2000 ]; % Frequency range

power = y.*conj(y)/n;   % Power of the DFT

plot(f,power)
xlabel('Frequency (Hz)')
ylabel('Power')
title('ERG Power Spectrum')
```

B.3 MATLAB Code for Short Time Fourier Transform

```
clc;
clear all;
close all;

%------------------------------------------------ ERG Signal

s=xlsread('RT_OD&OS_RF_WB_042215.xls'); % ERG Signal excel file

t=[0:0.5:225.5]; % TOTAL OF 452 points

fs=2000;

spectrogram(s,50,30,400,fs,'yaxis');

title('ERG Short Time Fourier Transform');
```

B.4 MATLAB Code for Continuous Wavelet Transform (Time vs. Scales)

```
clc;
clear all;
close all;

%------------------------------------------------ ERG Signal

s=xlsread('RT_OD&OS_RF_WB_042215.xls'); % ERG Signal excel file
```

```
t=[0:0.5:225.5];

fs = 2000;

s0=20000./2000;
scales=s0*(2.^(0:0.001:log2(length(s))));


F_scale=scal2frq(scales,'db10',1/fs);

coefs = cwt(s,scales,'db10','scalCNT');

[r1,c1]=size(coefs);

for k = 1: r1

coefs_norm(k,:)= coefs(k,:)./ (scales(k).^0.6);

end;

SC = wscalogram('contour',coefs_norm);
```

B.5 MATLAB Code for CWT Scales to Frequency Translation

```
clc;
clear all;
close all;

%------------------------------------------------ ERG Signal

s=xlsread(‘RT_OD&OS_RF_WB_042215.xls'); % ERG Signal excel file


t=[0:0.5:225.5];

fs = 2000;

s0=20000./2000;
scales=s0*(2.^(0:0.001:log2(length(s))));


F_scale=scal2frq(scales,'db10',1/fs);

coefs = cwt(s,scales,'db10','scalCNT');

[r1,c1]=size(coefs);

for k = 1: r1

coefs_norm(k,:)= coefs(k,:)./ (scales(k).^0.6);
```

```
end;

plot (scales , F_scale);

axis tight;

grid on;

xlabel('Scales');

ylabel('Frequency (Hz)');

title('Scales to Frequency Translation');
```

B.6 MATLAB Code for Continuous Wavelet Transform (Time vs. Frequency)

```
clc;
clear all;
close all;

%------------------------------------------------ ERG Signal

s=xlsread('RT_OD&OS_RF_WB_042215.xls'); % ERG Signal excel file


t=[0:0.5:225.5];

fs = 2000;

s0=20000./2000;
scales=s0*(2.^(0:0.001:log2(length(s))));


F_scale=scal2frq(scales,'db10',1/fs);

coefs = cwt(s,scales,'db10','scalCNT');

[r1,c1]=size(coefs);

for k = 1: r1

coefs_norm(k,:)= coefs(k,:)./ (scales(k).^0.6);

end;

contour(t,F_scale,abs(coefs_norm).^2);

axis tight;

grid on;
```

```
xlabel('Time');

ylabel('Approximate Frequency (Hz)');

title('CWT with Time vs Frequency');
```

B.7 MATLAB Code for Continuous Wavelet Transform (Cone of Influence)

```
clc;
clear all;
close all;

%------------------------------------------------ ERG Signal

s=xlsread(‘RT_OD&OS_RF_WB_042215.xls'); % ERG Signal excel file


t=[0:0.5:185];

fs = 2000;

s0=20000./2000;
scales=s0*(2.^(0:0.001:log2(length(s))));


F_scale=scal2frq(scales,'db10',1/fs);

coefs = cwt(s,scales,'db10','scalCNT');

[r1,c1]=size(coefs);

for k = 1: r1

coefs_norm(k,:)= coefs(k,:)./ (scales(k).^0.6);

end;

SC = wscalogram('contour',coefs_norm);
```

B.8 MATLAB Code for Castro’s ERG Model

```
%a-wave model

t_pos=[0:0.5/1000:225.5/1000]; % positive time in seconds

alpha1=1.178; % intensity factor

K1=-0.0018; % peak amplitude
```

```
tp=47/1000; %  peak time
mod1=((t_pos/tp).*(exp(1-(t_pos/tp))));
mod_p=mod1.^5; %mod1 raised to power 5
a_wave = K1*[1 - exp(-alpha1*mod_p)];
alpha1=1.178; % intensity factor
K1=-28; % peak amplitude
tp=16.5/1000; %  peak time
mod1=((t_pos/tp).*(exp(1-(t_pos/tp))));
mod_p=mod1.^5; %mod1 raised to power 5
a_wave = K1*[1 - exp(-alpha1*mod_p)];
a_wave = a_wave .* 1.47;
%b-wave model
K2=-0.6;
alpha2=1.1;
mod2=exp(-alpha2*t_pos).*(sin(30*t_pos));
b_wave=K2*t_pos.^3.*mod2;
a_wave_final = a_wave .* 25000;
b_wave_final = b_wave .* 50000;
erg=a_wave_final+b_wave_final;
plot (t_pos,erg);
```

APPENDIX C: COPYRIGHT APPROVAL LETTER

The ERG signal used in the analysis has been provided by Dr. Radouil Tzekov. The ERG signal was self-collected of Dr. Tzekov's right eye. The following letter shows the permission of use of the obtained ERG signal.

March 2016

LETTER FOR PERMISSION TO USE COPYRIGHTED WORKS

March 9, 2016

Dr. Radouil Tzekov

Dear Dr. Tzekov:

I am a graduate student in the Electrical Engineering Department at USF. I am in the process of preparing my thesis manuscript which is a requirement for my Master of Science in Electrical Engineering. I have been asked to seek your permission in order to include the ERG signal data that you have made available for analysis and publication.

Please indicate your approval of this request by providing the information requested below and your signature.

Very truly yours,

Abdulrahman Alaql
alaql@mail.usf.edu

For copyright owner use:

PERMISSION GRANTED FOR THE USE REQUESTED ABOVE:

By: Dr. Radouil Tzekov

Title: Assistant Professor

Date: 3/11/16